Deep-Sea Research II 55 (2008) 2068–2085

Contents lists available at ScienceDirect

Deep-Sea Research II

journal homepage: www.elsevier.com/locate/dsr2

Primary production within the sea-ice zone west of the Antarctic Peninsula: I—Sea ice, summer mixed layer, and irradiance

Maria Vernet [a,*], Douglas Martinson [b], Richard Iannuzzi [b], Sharon Stammerjohn [c], Wendy Kozlowski [a], Karie Sines [a], Ray Smith [d], Irene Garibotti [e]

[a] Integrative Oceanographic Division, Scripps Institution of Oceanography, MC 0218, University of California San Diego, La Jolla, CA 92093-0218, USA
[b] Lamont-Doherty Earth Observatory, Columbia University, Oceanography 105E, 61 Route 9W, Palisades, NY 10964, USA
[c] Department of Earth and Environmental Sciences, Columbia University, New York, NY 10027, USA
[d] Department of Geography, University of California, Santa Barbara, CA 93106, USA
[e] Instituto Argentino de Nivología, Glaciología y Ciencias Ambientales, C.C. 330, 5500 Mendoza, Argentina

ARTICLE INFO

Article history:
Accepted 24 April 2008
Available online 22 July 2008

Keywords:
Primary production
Sea ice
Mixed layer depth
Polar waters
Phytoplankton

ABSTRACT

In shelf waters of the western Antarctic Peninsula (wAP), with abundant macro- and micronutrients, water-column stability has been suggested as the main factor controlling primary production; freshwater input from sea-ice melting stabilizes the upper water column by forming a shallow summer mixed layer. Retreating sea ice in the spring and summer thus defines the area of influence, the sea-ice zone (SIZ) and the marginal ice zone (MIZ). A 12-year time series (1995–2006) was analyzed to address two main questions: (1) what are the spatial and temporal patterns in primary production; and (2) to what extent and in what ways is primary production related to sea-ice dynamics. Data were collected on cruises performed during January of each year, at the height of the growth season, within the region bounded by 64°S and 64°W to the north and 68°S and 66°W to the south. Average daily integrated primary production varied by an order of magnitude, from ~250 to ~1100 mg C m^{-2} d^{-1}, with an average cruise primary production of 745 mg C m^{-2} d^{-1}. A strong onshore–offshore gradient was evident along the shelf with higher production observed inshore. Inter-annual regional production varied by a factor of 7: maximum rates were measured in 2006 (1788 mg C m^{-2} d^{-1}) and minimum in 1999 (248 mg C m^{-2} d^{-1}). The results support the hypothesis that primary production in the wAP shelf is related to sea-ice dynamics. To first order, shallower summer mixed-layer depths in the shelf correlated with late sea retreat and primary production. Principal component analysis showed that high primary production in January was associated with enhanced shelf production toward the coast and in the south, explaining 63% of the variability in space and time. This first mode captured the inter-annual variability in regional production. Temporal variability in primary production (time series of anomalies defined for each location) showed spatial dependence: higher primary production correlated with shallow mixed-layer depths only at mid-shelf; in coastal and offshore waters, primary production correlated with deeper mixed layers. Thus, coastal primary production can show a non-linear relationship with summer mixed layers. Under conditions of large biomass (>20 mg chl *a* m^{-3}) and shallow mixed-layer depth (e.g., 5 m) phytoplankton production becomes light limited. This limitation is reduced with a deepening of the summer mixed layer (e.g., 20 m). Dominance of diatoms and the ability to adapt and photosynthesize at higher light levels characterized the large phytoplankton blooms. No significant regional trend in primary production was detected within the 12-year series. We conclude that the regional average primary production on the wAP shelf is associated with shallow summer mixed layers in conjunction with late sea-ice retreat. An opposite relationship is observed for the highest production rates in coastal waters, associated with large biomass, where a deepening of the summer mixed layer relieves light limitation.

1. Introduction

The average primary productivity in the west of the Antarctic Peninsula (wAP) region is estimated around 182 ± 107 g C m^{-2} y^{-1}, which is a factor of 4 lower than other productive coastal areas of

* Corresponding author. Tel.: +1 858 534 5322; fax: 1 858 822 0562.
E-mail addresses: mvernet@ucsd.edu (M. Vernet), wkozlowski@ucsd.edu (W. Kozlowski).

0967-0645/$ - see front matter © 2008 Elsevier Ltd. All rights reserved.
doi:10.1016/j.dsr2.2008.05.021

world's oceans (Vernet and Smith, 2006) and similar to other shelf areas in Antarctica (Arrigo et al., 1998), but higher than the productivity at the Polar Front (Moore and Abbott, 2000). Phytoplankton biomass in the wAP region starts to accumulate in October triggered by the increase in day length. Mean chlorophyll *a* (chl *a*) in the surface 30 m can increase from o 0.5 mg m^{-3} in a pre-bloom period, to higher than 15 mg m^{-3} during a bloom, with average concentrations between 1 and 3 mg m^{-3} (Smith et al., 2008). In January, at the peak of the growth season, phytoplankton cell abundance, carbon biomass, and chl *a* concentrations show great variability along an on/offshore gradient. The gradient in chl *a* concentration, varying from an average concentration of 4.22 mg chl *a* m^{-3} in the coastal region to 0.83 and 0.26 mg chl *a* m^{-3} in the middle shelf and slope waters, respectively, is a consistent feature from year to year (Smith et al., 1996, 1998a, b; Garibotti et al., 2005a).

Annual productivity in the wAP is thought to be dominated by the high production rates associated with blooms, whose development may be timed and paced by water-column stability as induced by, for example, sea-ice meltwater (Smith and Nelson, 1986; Mitchell and Holm-Hansen, 1991; Sakshaug et al., 1991), favorable meteorological conditions (Smith et al., 1987b; Lancelot et al., 1993; Smith et al., 1998a, b), and/or glacier meltwater later in the season (Dierssen et al., 2001). Oceanic waters are believed to be limited mainly by light, micronutrients such as Fe (Martin et al., 1990a; Boyd et al., 2000; Coale et al., 2004), or microzooplankton grazing (Burkill et al., 1995). Episodic blooms might be associated with intrusions of the southern boundary of the Antarctic Circumpolar Current (ACC) on the wAP shelf (Boyd et al., 1995; Savidge et al., 1995) and/or upwelling at the shelf break (Prézelin et al., 2000).

In shelf waters of the wAP, with abundant macro- and micronutrients (Martin et al., 1990b), water-column stability has been suggested as the main factor controlling primary production (Mitchell and Holm-Hansen, 1991; Tréguer and Jacques, 1992). Freshwater input from sea-ice (or glacial) meltwater is recognized as the principal factor in stabilizing the upper water column by forming a shallow summer mixed layer (SML) over winter water (Klinck, 1998; Walsh et al., 2001; Garibotti et al., 2003a). Melting sea ice can seed the newly formed SML with sea-ice algae, a factor believed to enhance phytoplankton growth at the ice edge (Ackley and Sullivan, 1994). The algae are incorporated into sea ice by the entrainment of phytoplankton in the water column during frazil ice production in the fall (Garrison et al., 1983), followed by *in situ* growth during winter and early spring (Fritsen et al., 1998). Early ice formation (advance) in the fall is expected to maximize algae entrainment and late and/or protracted ice retreat in the spring is expected to create shallow mixed layers exposed to increasing sunlight and day length. Such conditions are thought to be ideal for phytoplankton growth at the ice edge during the following growth season.

A key hypothesis of the Palmer Long-Term Ecological Research (LTER) program is that the annual advance and retreat of sea ice is a major physical determinant of spatial and temporal changes in the structure and function of the Antarctic marine ecosystem. The linkage of seasonal sea-ice dynamics to primary production is one of the principal routes by which physical forcing modulates the wAP ecosystem. Earlier studies have linked the seasonal progression of phytoplankton to ice conditions from the previous winter (Smith et al., 1998, 2001; Garibotti et al., 2005a). In this paper we test the degree of control, in space and time, which sea-ice dynamics imposes on primary production based on a 12-year time series from 1995 to 2006. Our working hypothesis is that the timing of sea-ice formation and retreat is an important determinant of summer primary production. Several sea-ice characteristics were defined that capture different properties of the annual sea-ice cycle and serve as a single (yearly) sea-ice parameter that can be compared to biological parameters across space and time (Stammerjohn et al., 2008). The three sea-ice characteristics used in this study are: (1) the timing of sea-ice advance, (2) the timing of sea-ice retreat, and (3) sea-ice persistence (the percent time sea ice is present between the initial advance and final retreat). The spatial and temporal analysis of primary production and sea-ice dynamics will address two main questions: (1) what are the spatial and temporal patterns in primary production; and (2) to what extent and in what ways is primary production related to sea-ice dynamics.

2. Methods

2.1. Sampling

Samples for the estimation of phytoplankton primary production were collected over the continental shelf wAP on board the R.V. *Polar Duke* (1995–1997) and the A.R.S. V. *Laurence M. Gould* (1998–2006). Cruises were during January of each year, within the region bounded by 64°S and 64°W to the north and 68°S and 66°W to the south (Waters and Smith, 1992; Fig. 1). During each cruise about 43–53 stations (up to 67) were sampled along five cardinal lines (600–200) perpendicular to the Antarctic Peninsula, extending from the coast to slope waters within Anvers Island and Marguerite Bay, in a northwest (NW) to southeast (SE) direction.

2.2. Primary production

Estimates of primary production were made experimentally at each station, with samples taken from 10-l Niskin or 12-l Go-Flo bottles attached to the ship's conductivity–temperature–depth (CTD) rosette. To estimate production within the euphotic zone, water was sampled from depths corresponding to 100%, 50%, 25%, 10%, 5%, and 1% of incident irradiance. *In situ* irradiance was measured at each station to determine the sampling depths; a bio-optical profiler BOPS-II (Smith and Nelson, 1985) was used from 1995 to 1997, a QSL-200 was attached to the CTD rosette

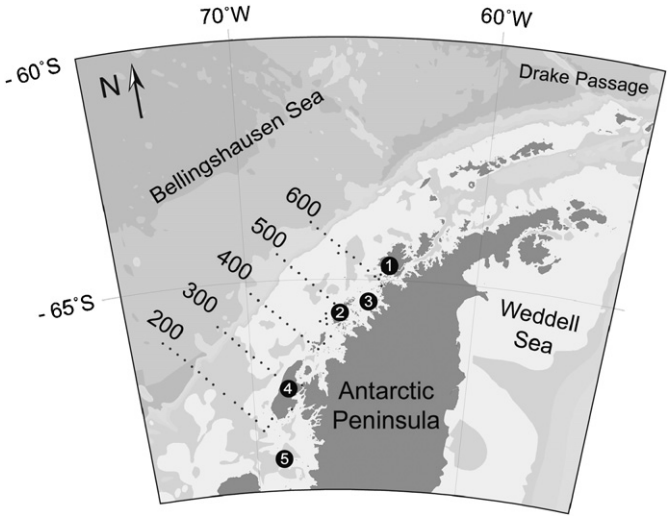

Fig. 1. Map of the study area depicting the grid lines (100 km apart) sampled by the Palmer Long-Term Ecological Research project in the west of the Antarctic Peninsula. Grid lines are labeled from 600 (furthermost north off Anvers Island) to 200 (off Marguerite Bay). Dots in the grid lines represent stations (20 km apart). January cruises (1995–2006) routinely sampled these five transect lines. Topography is shown in background gray. The shelf is 200-km wide with an average depth of 500 m. (1) Anvers Island (where Palmer Station is located), (2) Renaud Island, (3) Grandidier Passage, (4) Adelaide Isl and (5) Marguerite Bay.

from 1998 to 2000, and a PRR-600 or PRR-880 was used from 2001 to 2006 (Biospherical Instruments Inc.). Samples were collected during day time, usually between 5 am and no later than 10 pm (day length was approximately 18 h during cruises).

Primary production was estimated during 24-h on-deck incubations in UV opaque plexiglas (UV-O) tubes placed in a shade-free area, with temperature maintained at surface *in situ* conditions by running sea water. Duplicate 100-ml samples were exposed to surface solar irradiance in 125-ml borosilicate bottles after addition of 5 μCi of $NaH^{14}CO_3$ per bottle (light bottles). Parallel incubations were kept in the dark (dark bottles). After 24 h, the samples were concentrated onto 25-mm Whatman GF/F filters, fumed with 20% HCl for 24 h and placed in 5 ml of Universol ES scintillation fluid. Radioactivity in the samples was counted on a scintillation counter (Wallac 1414 or 1210). Specific activity of each sample was determined from 0.1 ml of seawater after ^{14}C inoculation. Time-zero values, determined from filtration of a 100-ml sample before incubation, were always o 5% of the light data. Primary production was calculated from the difference of light- and dark-bottle readings and assuming a HCO_3^- in the water of 24,000 mg C kg^{-1} (Carrillo and Karl, 1999).

Primary production is expressed as daily primary production integrated to the depth of the euphotic zone in units of mg C m^{-2} d^{-1}. The euphotic zone (Z_{eu}) was defined as the depth of 1% intensity of surface irradiance measured at each station (as photosynthetically available radiation—PAR, l = 400–700 nm).

2.3. Sea-ice estimates and calculation of sea-ice parameters

Satellite measurements of sea-ice concentration are from NASA's Scanning Multichannel Microwave Radiometer (SMMR) and the Defense Meteorological Satellite Program's (DMSP) Special Sensor Microwave/Imager (SSM/I). Sea-ice concentrations were determined using the bootstrap passive microwave algorithm (Comiso, 1995), from which a SMMR-SSM/I time series was created (used here: January 1, 1994–December 31, 2005), which minimizes the differences between the various SMMR and SSM/I sensors (Comiso et al., 1997). The every-other-day SMMR and the daily SSM/I sea-ice concentration data were provided by the EOS Distributed Active Archive Center (DAAC) at the National Snow and Ice Data Center, University of Colorado in Boulder, Colorado (http://nsidc.org). For this analysis, a set of sea-ice characteristics (defined below) were determined from the sea-ice concentration data within the SMMR-SSM/I polar stereographic grid space; those data were then re-binned into an equal-area Palmer LTER grid to facilitate direct comparisons with the biological data.

Three independent sea-ice characteristics (day of advance, day of retreat, and ice persistence) were determined from the (quasi) daily images of SMMR-SSM/I sea-ice concentration (Stammerjohn et al., 2008). The year days of advance and retreat were determined at each grid point and for each sea-ice year (defined here to begin and end at the mean summer sea-ice extent minimum as observed in the Palmer LTER region: March 15 of current year to March 14 of following year). Day of advance was defined as the first day of the first 5-day sequence with sea-ice concentration greater than 15% (or, for comparison, 50%). Day of retreat was defined as the day when sea-ice concentration decreased past the given threshold and remained below that threshold until the end of the sea-ice year. Openings can be created within the pack ice during periods of wave-generated (tidal or wind-driven) divergence and/or ocean–ice interactions. This difference was captured by the last sea-ice characteristic, sea-ice persistence, which is the percent time sea ice is present within the interval between day of advance and retreat.

2.4. Data analysis

The biological data were binned into an equal-area grid with cell size of 40 km (onshore–offshore) by 100 km (along shore). When we present the gridded spatial maps of primary production, for example, white dots indicate the actual location of data within each grid cell. Spatial data gaps across the grid in particular years are filled, when necessary (e.g., for comparing data fields) following the reduced-space optimal analysis (OA) of Kaplan et al. (1997).

Data on the rates of primary production are characterized by a log-normal (ln) distribution of non-zero values, and a high variance in the log distribution called a delta distribution (DD; Aitchison, 1955). It has been shown that for zooplankton data, estimates of the mean and variance based on the delta distribution DD are better than the ordinary sample mean (Pennington, 1983; Gilbert, 1987), and we have chosen to use it as well for phytoplankton. The following equations were used to calculate the mean (c) and variance (var_{est} (c)) of abundance data with a sample size of n, and m non-zero values ($x_1,\ldots,x_m$) where y and sy^2 are the sample mean and variance, respectively, of the natural log of the non-zero values, and t is half the variance, i.e. $t = sy^2/2$:

$$
\begin{aligned}
c &= (m/n)\exp(y)G_m(t) \quad \text{when } m>1,\\
&= x_1/n \quad \text{when } m=1; \quad \text{and}\\
\mathrm{var}_{\mathrm{est}}(c) &= (m/n)\exp(2y)\{(m/n)Gm^2(t)\\
&\quad -((m-1)/(n-1))G_m(sy^2(m-2)/(m-1))\}\\
&\quad \text{when } m>1,\\
&= (x_1/n)_2 \text{ when } m=1.
\end{aligned}
$$

The factor G_m is calculated with the following progression, based on m and sy^2:

$$
\begin{aligned}
G_m(t) &= 1+((m-1)t)/m+((m-1)^3t^2)/(2!m^2(m+1))\\
&\quad +((m-1)^5t^3)/(3!m^3(m+1)(m+3))+\cdots
\end{aligned}
$$

and also can be found in the tables of Aitchison and Brown (1957). If zero values are not present, $m=n$, $m/n=1$, and the series converges.

We explore spatial–temporal patterns in the data via classical principal component analysis (PCA), which decomposes the data into orthogonal modes. The first (gravest) mode describes the most amount of data variance, and the second mode the most of the remaining unexplained variance, etc. until all of the variance in the data has been described. While this is a statistical procedure, it works on the idea that "signal" tends to manifest itself in meaningful or coherent structure, and thus the lowest order modes are hoped to describe biologically meaningful structure, whereas the highest order modes describing little overall variance are simply noise, or isolated structure. Each mode is described by a spatial pattern (the empirical orthogonal function, or EOF) and a principal component (PC), a time series describing the change in amplitude of the EOF through time. The modes are orthogonal and add to 100% of the total variance. Focus on the lowest order modes presumably gives an improved signal-to-noise ratio, best extracting useful information, but this is not guaranteed. The details of the procedures, and necessary optimal analysis OA required to fill (interpolate) gaps in the original data, are presented in Martinson et al. (2008). While the anomalies that are shown and discussed are defined as the data minus its climatology (as defined above for DD data), what was decomposed for the PCA is the ln of the data minus the mean of the ln of the data. Thus, meanless, normally distributed data was decomposed as desired for the PCA. Correlation maps were estimated by correlating interpolated sea-ice variables against

primary production time series, in each grid cell, presented as *r*. The trend represents the robust least squares fit of the data decomposed for the PCA (i.e. data is normally distributed). Significance was defined as $Z > 11.96$, where Z is defined as the regression coefficient (r) divided by the standard error of the fit of each grid cell.

The daily integrated primary production is compared to the previous winter's sea-ice data (i.e. it is lagged 1 year), since the ice season was defined by calendar year (15 March of the present year to 14 March of the following year, see Section 2.3), and primary production was sampled in January and February of the following year.

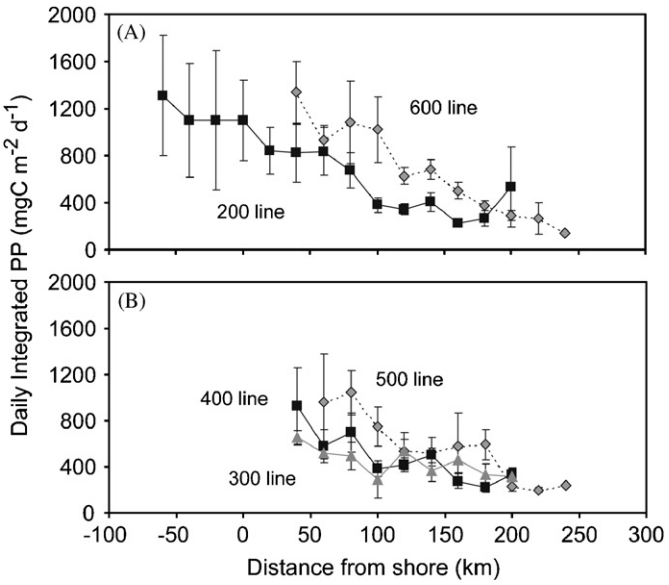

Fig. 2. Spatial distribution of integrated daily primary production (PP), in mg C m^{-2} d^{-1}, as average ±95% confidence interval (CI) within the euphotic zone (surface to depth of 1% incident irradiance). Estimates obtained once per year at each location with 24-h incubations. *X*-axis defines the average distance from the peninsula in kilometers (km). Stations inside Marguerite Bay are depicted as negative; (A) 600 and 200 transect lines; (B) 500, 400, and 300 transect lines.

3. Results

Primary production was distributed along an onshore–offshore gradient with higher production inshore (Fig. 2). Although the magnitude of the gradient was not constant, the pattern was consistent along the study area and matches previous descriptions of biomass between 62°S and 64°S (Smith et al., 1996). Variability was high, in particular in inshore waters.

3.1. Primary production

Combining all cruises, we generated a spatial climatology map describing the distribution of the summer daily integrated primary production for the 12-year series (Fig. 3A). Average rates varied by an order of magnitude, from ~250 to ~1100 mg C m^{-2} d^{-1}. The pronounced onshore–offshore gradient defined an area of higher production at the inner shelf in the north, west of Anvers and Renaud Islands, and close to the coast in the center and south, with the exception of the area west of Adelaide Island. Shelf production, shoreward of the continental slope, presented intermediate values, at ~500 to 750 mg C m^{-2} d^{-1}. Over the continental slope, daily integrated production rates were consistently lower, between 250 and 400 mg C m^{-2} d^{-1}. The steepest onshore–offshore gradient was observed in the South, off Marguerite Bay, which presented the lowest daily production rates on slope waters and highest at the mouth of the bay.

The variability in daily integrated primary production rates was higher inshore, coincident with areas of higher average production, with the exception of Grandidier Passage, east of Renaud Island. For any given area, the coefficient of variation

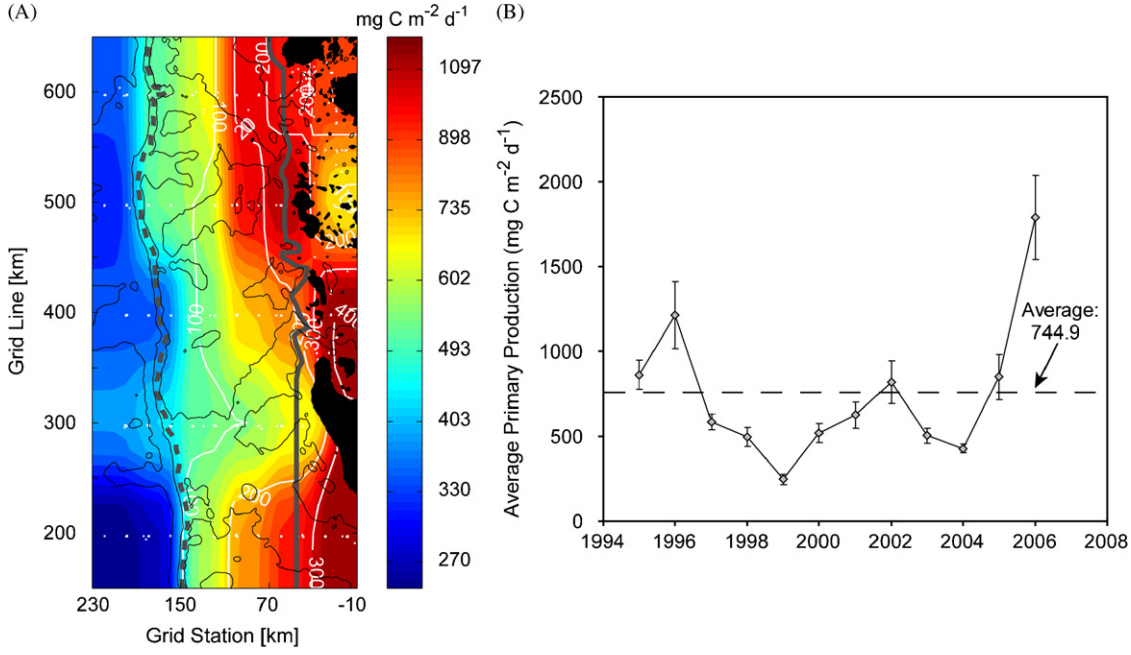

Fig. 3. Daily integrated primary production (mg C m^{-2} d^{-1}; 1995–2006). (A) Twelve-year spatial climatology map, calculated as the average value of the times series at each location; with standard deviation (white lines). Bottom topography (thin black lines) and water masses (slope, shelf, and coastal, thick gray lines; Martinson et al., 2008) are indicated. White points indicate location of the stations sampled. (B) Average cruise (January) daily integrated primary production (arithmetic mean). Bars correspond to standard error, n~43 stations. Horizontal line depicts the 12-year arithmetic mean of 745 mg C m^{-2} d^{-1}.

(standard deviation/average, Fig. 3A) was between 25% and 40% of daily rates, with higher variation in slope waters.

3.2. Ice indexes and mixed-layer depth

Similar to the primary production, climatology maps of the ice distribution (e.g., ice indexes) and SML depth showed the distribution of average values for the area in the 12-year series (Fig. 4). Sea ice started forming in inshore waters close to Anvers Island (Fig. 4A; year day 90–120, April), somewhat later in the SW area of Marguerite Bay (year day 130–150, late May), and formed last at mid-shelf and offshore waters (year day 150–190, in June and early July). During the following spring and summer, ice started melting in offshore waters (Fig. 4B; year day 300–320, in early November), continued at mid-shelf (year day 340, in early

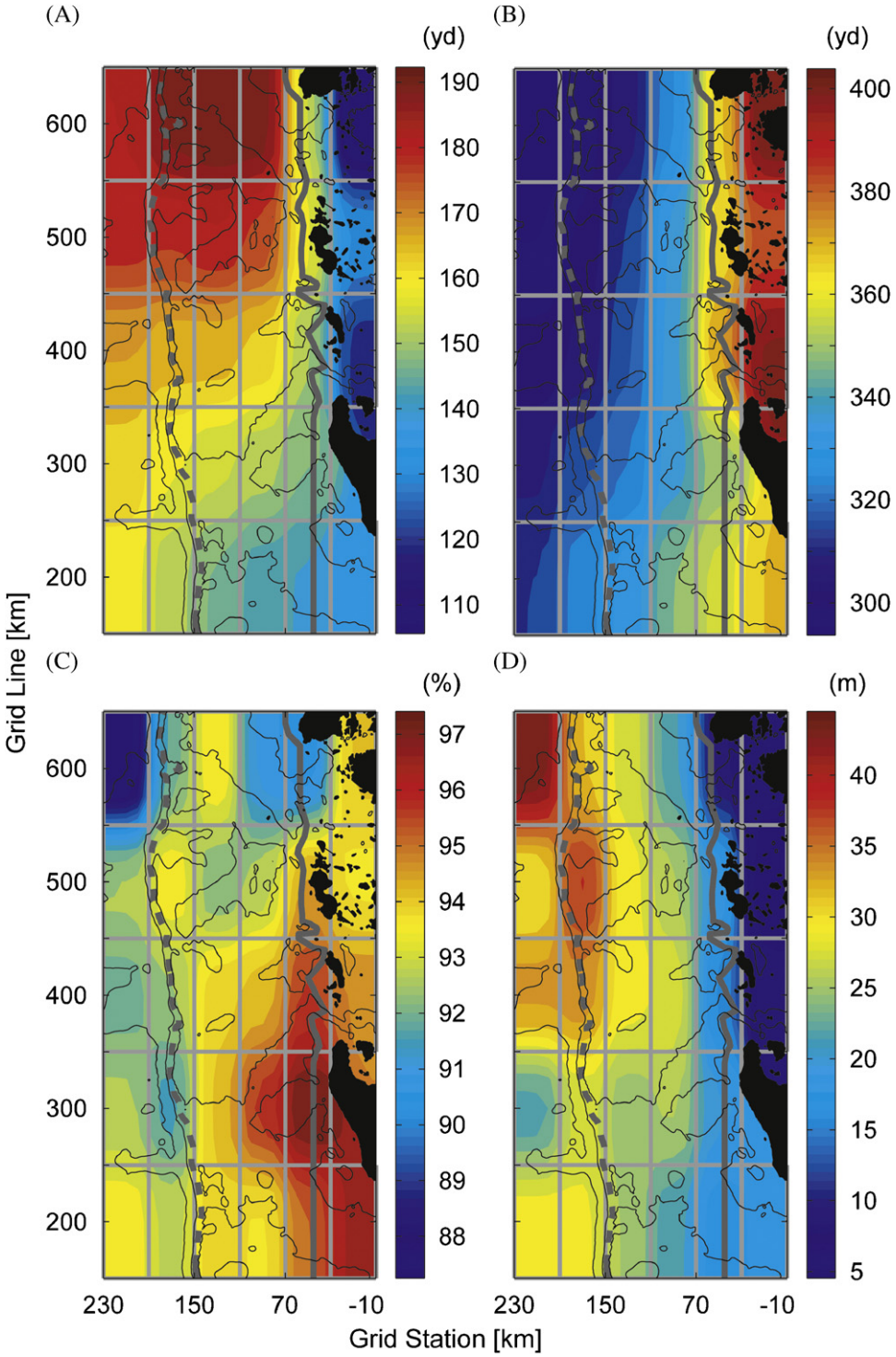

Fig. 4. Spatial climatology map of environmental variables: (A) timing of sea-ice advance, in year days (YD), (B) timing of sea-ice retreat, in YD, (C) sea-ice persistence through the winter, in %, and (D) summer mixed-layer depth (SML) in m. Definition of the ice indexes can be found in Section 2.3 of Methods. YD > 365 are based on days after 1 January (i.e. 1 January is year day 366) as the ice season is calculated from 15 March to 14 March of the following year.

December) and was melted last in inshore waters of Marguerite Bay (year day 360, at the end of December) and north in the coast in the middle of the summer (year day 380–400, in late January and early February). Ice persistence was higher in coastal and mid-shelf waters of the south, with almost constant ice cover once it was formed (96–98%; Fig. 4C). Decreasing persistence was found toward the north and offshore waters (i.e. ice stayed ~85% of the time once was formed).

The depth of the SML, thought to be established during sea-ice retreat in spring and summer, and modified by solar heating and turbulent wind mixing, showed during the study period a strong onshore–offshore gradient in its spatial climatology (Fig. 4D). Deeper mixed layers were present in slope waters (30–40 m) and shallow mixed layers (5–15 m) were found, on average, in coastal waters, close to sea ice (i.e. the marginal ice zone (MIZ) in summer, Fig. 4D).

The daily integrated primary production in January correlated positively with the timing of sea-ice retreat during the previous spring (Fig. 5A; $R^2 = 0.58$, $n = 29$) and negatively with the depth of the SML (Fig. 5B, $R^2 = 0.45$, $n = 29$). SML correlated with the timing of sea-ice retreat in support of the hypothesis that melting sea ice is responsible for water-column stratification in the region ($R^2 = 0.83$, Fig. 5C; see also Stammerjohn et al., 2008). The relationship of average daily integrated primary production with timing of sea-ice advance or sea-ice persistence was comparatively low ($R^2 = 0.13$ and $R^2 = 0.04$, respectively; data not shown).

3.3. Temporal and spatial variability

3.3.1. Inter-annual variability in summer primary production, 1995–2006

By subtracting the climatology mean from the measured value at each location (grid cell) we generated a yearly anomaly. Maps of the anomalies showed that the range of production in any given year and location varied by up to three orders of magnitude with respect to the climatology (Fig. 6). Notable large excursions from mean values were observed close to the coast in the Palmer Station area off Anvers Island in 1996, in the mouth of Marguerite Bay in 2002, or almost everywhere in 2006. Maximum regional production was observed in 2006 and minimum in 1999, corresponding to cruise averages of 1788 and 248 mg C m^{-2} d^{-1}, respectively ($n = 43$; Fig. 3B). Variability was high, with as much as ~1000 g C m^{-2} d^{-1} associated with the positive anomaly of 2006 or 500 mg C m^{-2} d^{-1} lower in the negative anomaly of 1999.

3.3.2. Anomaly correlation maps and environmental variables

By combining the yearly anomalies at each site we generated an anomaly time series for each variable. A comparison of these time series generated correlation maps for each pair of variables. We established relationships between the variability of primary production, the ice indexes, and SML depth in different areas. In this and subsequent comparative analysis, the primary production and SML depth were lagged by 1 year when comparing with sea-ice indexes, e.g., the production of January 1996 (representing the 1995–1996 growth season) was compared to the ice index of 1995 (determined from 15 March 1995 to 14 March 1996).

The features in PCA analysis, e.g., the correlation maps presented in Fig. 7, are taken as indications of the type of relationships that can exist in the field. An area is identified as notable by the strength of the correlation, the size of the feature, or the consistency with which the feature re-appears in different analyses. For example, Fig. 7A shows positive correlation between daily integrated primary production and the timing of sea-ice retreat anomalies in coastal and offshore waters. The positive ($r = 0.6$) correlation between sea-ice retreat and primary production in the Palmer area (inshore 600 line) would suggest that the production in January is high/low when sea-ice retreat is late/early while the area in the coast of the 500 line, immediately south, is not ($r = -0.1$). An absence of correlation can mean that production in January is related to other factors other than sea-ice retreat or that the effect of sea-ice retreat, present earlier in the season, is not detected any longer in January. The coastal area in the 500 line, east of Renaud Island, is rather anomalous in several physics, ice, and biology properties. For example, it was identified as an area of high grazing in January of 1997 (Garibotti et al., 2003b); large quantities of brash ice can accumulate in the summer; the phytoplankton community is frequently dominated by small flagellates, with a notable absence of diatoms. Thus, anomalies in one grid cells are not considered, unless the feature is consistent (e.g., the inner shelf in the 500 line, 500.090, Figs. 7B, 11B, and 12B).

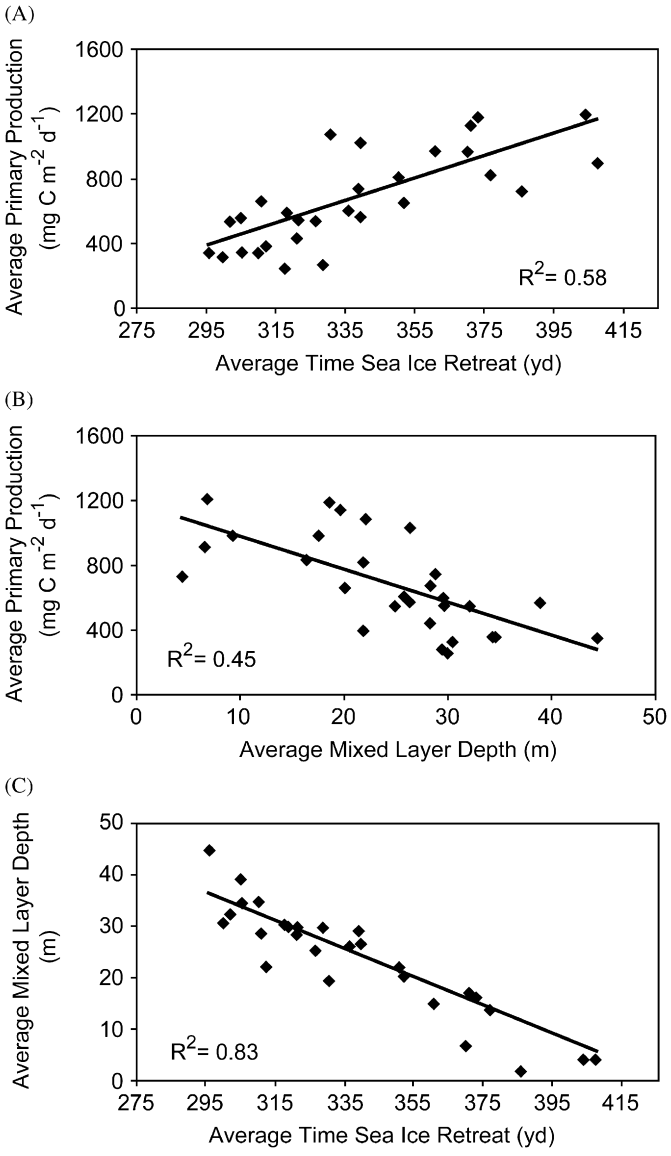

Fig. 5. Correlation between the average daily integrated primary production and average values of the environmental variables based on each grid cell (values extracted from Figs. 3A and 4). (A) Primary production vs. timing of sea-ice retreat (PP = 6.93(sea-ice retreat)−1670, $r^2 = 0.57$, $n = 29$); (B) primary production vs. summer mixed-layer depth (PP = −20.33SML+1173, $r^2 = 0.45$, $n = 29$); (C) summer mixed-layer depth vs. timing of sea-ice retreat (SML = −0.27(sea-ice retreat)+117, $r^2 = 0.83$, $n = 29$).

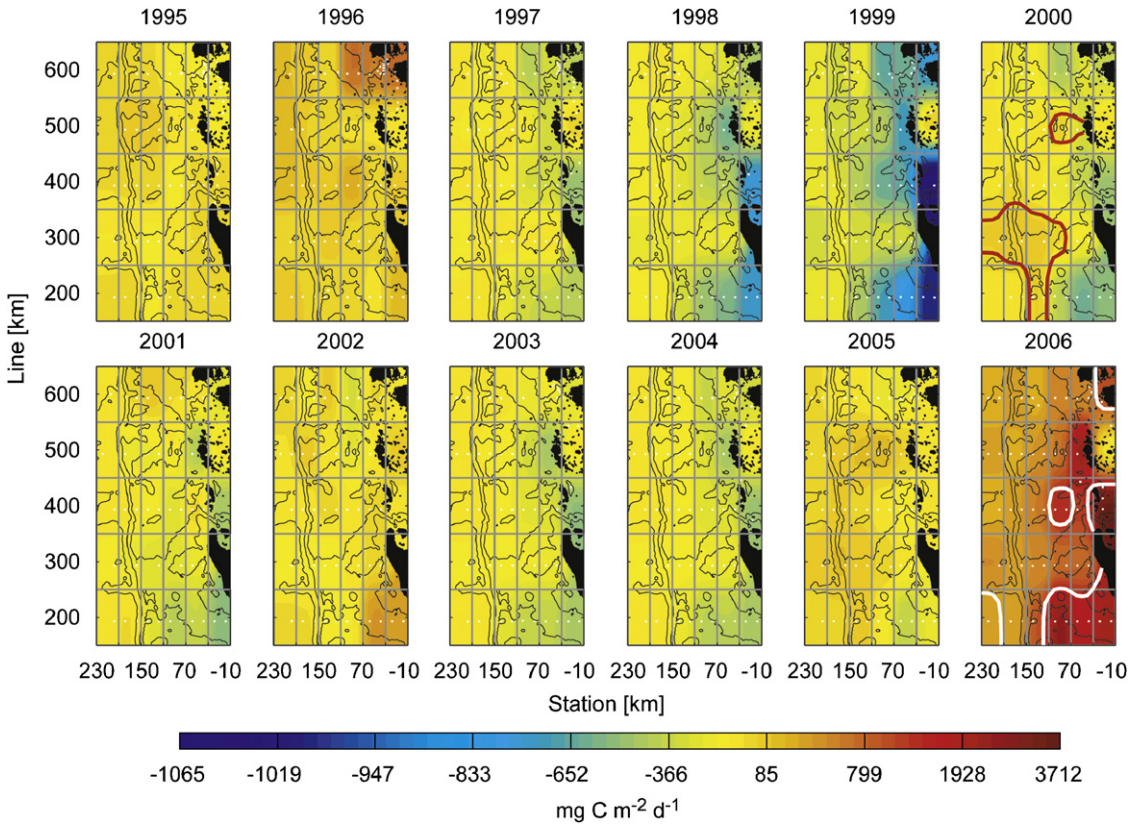

Fig. 6. Anomaly map of the daily integrated primary production (annual value—the 12-year climatology at each grid cell, per year). Color bar depicts primary production in $mg\,C\,m^{-2}\,d^{-1}$: yellow shows average distribution (i.e. 2005), blue depicts negative anomalies (i.e. coastal waters in 1999), and red indicates high positive anomalies (i.e. coastal waters in 2006). An overlay showing expression of the first empirical orthogonal function (EOF) for primary production in year 2006 (white line) and second EOF in year 2000 (red line), as shown in Fig. 8.

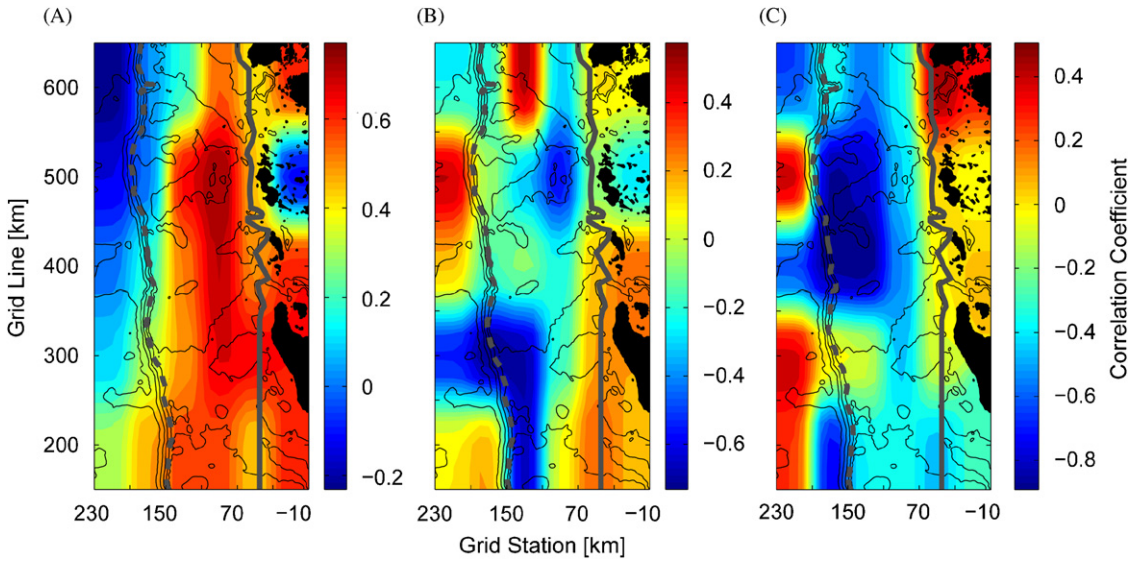

Fig. 7. Spatial correlations maps between daily integrated primary production and environmental variables, calculated based on the time series of the anomalies at each grid cell, for two variables of interest, where areas of positive correlation are depicted in red (see color bar on the right of each figure). (A) Primary production and timing of sea-ice retreat; (B) primary production and summer mixed-layer depth; and (C) timing of sea-ice retreat and summer mixed-layer depth. Note color scales differ between plots.

Correlation between the variability of primary production, the timing of sea-ice retreat, and SML depth showed large spatial dependence (Fig. 7). Shelf and coastal waters indicate high daily integrated primary production during late sea-ice retreat or low primary production during early sea-ice retreat (Fig. 7A). No correlation was seen in offshore waters, suggesting no or low influence of sea-ice dynamics in the spring with local summer primary production. As concluded by Smith et al. (2008), high spring (November) biomass just offshore of the shelf break can be attributed to the Southern Antarctic Circumpolar Current Front

(SACCF). The results presented here emphasize the possible role of SACCF later in the season.

The variability in primary production at mid-shelf correlated negatively with variability in the depth of the SML ($r = -0.2$ to -0.6). As expected, and similar to what was observed for average values in this area (Fig. 5B), high/low primary production was related to shallow/deep SML. In contrast, coastal and slope waters showed neutral or positive correlation, where high/low primary production was seen in deep/shallow SML ($r = 0.2$–0.4). The shallower SML at the shelf correlated with late sea-ice retreat along most of the mid-shelf (Fig. 7C; $r = -0.5$ to -0.7). Variability in SML in coastal and offshore area was either neutral (yellow) or positive (red or orange), with deep/shallow SML corresponding to late/early sea-ice retreat, thus capturing a correlation opposite in sign to that of the climatologies (Fig. 5C).

In summary, although average values of primary production, SML depth, and timing of sea-ice retreat correlated as expected from previous studies, a more detailed analysis of the time series indicated that the variability among these variables can show the opposite relationship in coastal and slope waters.

3.3.3. *Main modes of variability in primary production and environmental variables*

A more in-depth analysis of the main modes of spatial and temporal variability in the variables of interest can help discover patterns in their complex inter-relationships. For that purpose we performed PCA, as shown below.

3.3.3.1. First mode of variability. The spatial pattern of the PC is shown in the corresponding EOF. The first or gravest mode in daily integrated primary production showed that the most common pattern of variability in the 12-year series was related to production in the southern and coastal areas, both for higher (1996, 2002, 2005, and 2006) and lower (1998, 1999) production (PC1, Fig. 8A). This mode indicated that 62% of the spatial variance in primary production in January was due to variance in production along the shelf in the 200 and 400 grid lines, offshore in the 200 line, and in coastal areas, from the 400 to the 200 grid lines (EOF1, Fig. 8D). In summary, there was a north–south gradient in co-variability

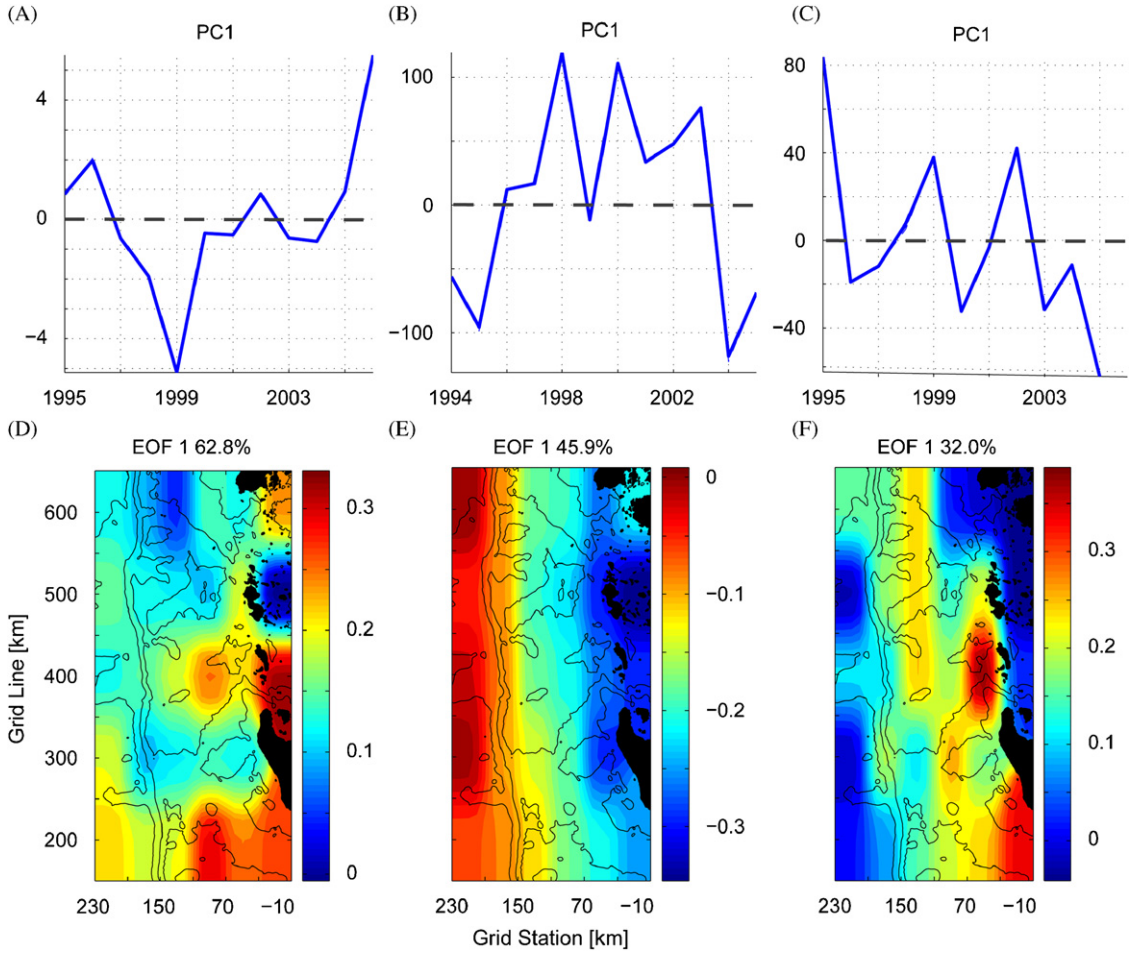

Fig. 8. Principal component analysis showing the first modes extracted, where each mode is defined by a time series (Principal Components (PC), shown in the top panels) and empirical orthogonal function maps (EOF, shown in the lower panels): (A) first principal component for daily integrated primary production; (B) first principal component for timing of sea-ice retreat; (C) first principal component for summer mixed-layer depth; (D) first EOF for primary production indicating the areas of variability in the years identified in PC1 (red areas indicate high for 1996, 2002, and 2006 and low for 1999, 2003, and 2004). EOF1 captures 63% of primary production variability. Note that the scale in EOF1 is always positive. See year 2006 in Fig. 6 as an example. (E) Spatial variability of first mode in sea-ice retreat (EOF1, explaining 47% of variability) in the years identified in PC1 (red shows no change, blue indicates areas of earlier sea-ice retreat in 1998, 2000, and 2003 and later sea-ice retreat in 1995, 2004, and 2005. (F) Spatial variability of first mode in summer mixed-layer depth (EOF1, explaining 32% of variability) in the years identified in PC1 (blue shows no change, red indicates areas of shallower mixed layers in 1996, 2000, 2003, and 2005 and deeper mixed layers in 1995, 1999, and 2002. *Note*: (1) color bars are different for the different variables. (2) The value of the color shown in the EOF map is a multiplier in the PC1 value for that location. (3) The positive/negative values in the EOF and PC plots are arbitrary. Analysis of the anomaly maps is needed to ascertain the modal signs (see Fig. 6).

where production in the south increases/decreases and all other areas do not.

The first or gravest mode in the timing of sea-ice retreat, capturing 47% of the spatial covariance -variance through time, showed that the most common pattern of variability was related to early/late timing in sea-ice retreat in coastal waters with respect to no variability in offshore waters (EOF1, Fig. 8E). Later sea-ice retreat was observed in 1998, 2000, and 2003 (PC1, Fig. 8B), and later retreat in 1995, 2005, and 2006.

The first or gravest mode in the depth of SML, capturing 32% of the spatial variance through time, showed that the most common pattern of variability from 1995 to 2006 was related to shallow/deeper depths along an area that extended from SE to NW (shown in red and orange) with respect to no co-variability in other areas (depicted in blue; EOF1, Fig. 8F). Shallower SMLs were observed in the mouth of Marguerite Bay and at mid-shelf in 1996, 2000, 2003, and 2005 and deeper SML in 1995, 1999, and 2002 (PC1, Fig. 8C). This mode indicated that the highest variability in SML corresponded to changes at mid-shelf and the SE area.

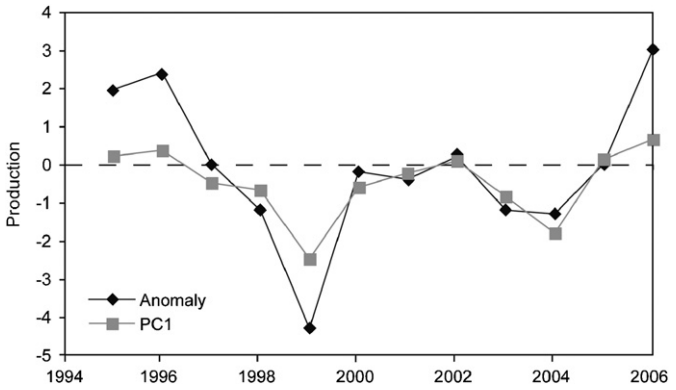

Fig. 9. Anomalies of daily average primary production in the wAP in January ($n = 43$ stations, 1-year lag) compared with the time development of the first principal component in primary production (PC1); correlation coefficient $r^2 = 0.83$.

The PC in the first mode of primary production (Fig. 8A) represented the inter-annual in regional primary production (Fig. 9). Positive anomalies were observed in 1995, 1996, and 2006 coinciding with positive PC1 values in the same years. Negative anomalies and negative PC1 values were observed in 1998, 1999, 2003, and 2004.

Temporal correlation in first modes of variability: The correlation between the PCs of the ice indexes, SML, and primary production was used to estimate the years of co-variability among the variables (Fig. 10). The first mode in primary production showed high temporal correlation with the first mode of timing of sea-ice retreat ($R^2 = 0.50$, Fig. 10A). Thus, during high/low production years, variability in the south (Fig. 8D) correlated with late/early sea-ice retreat within 70 km from shore (Fig. 8E). The years when this correlation was strongest were 3 years of high production (1995–1996, 2001–2002, and 2005–2006) and two of low production (1998–1999 and 2003–2004). Temporal variability in SML was correlated with the timing of sea-ice retreat, where 1995–1996, 1998–1999, and 2003–2004 had shallower SML and late sea-ice retreat (Fig. 10B; $R^2 = 0.58$). These shallower SML did not support higher primary production ($R^2 = 0.10$, data not shown).

Spatial correlation in first modes of variability: To understand the locations where the PC of one variable may affect another one, we generated correlation maps of the time series of the PC of one variable with the time series of the anomaly of the second variable. As expected, the first PC of the primary production and the anomalies of the timing of the sea-ice retreat correlated positively at mid-shelf and coastal waters (Fig. 11A), while the first PC of the SML correlated negatively with the anomalies of the timing of sea-ice retreat, for most of the study area (Fig. 11C). In contrast, and similar to the correlation of the anomalies (Fig. 7B), the time series of the first PC of the SML correlated negatively with the primary production anomalies at two main locations in

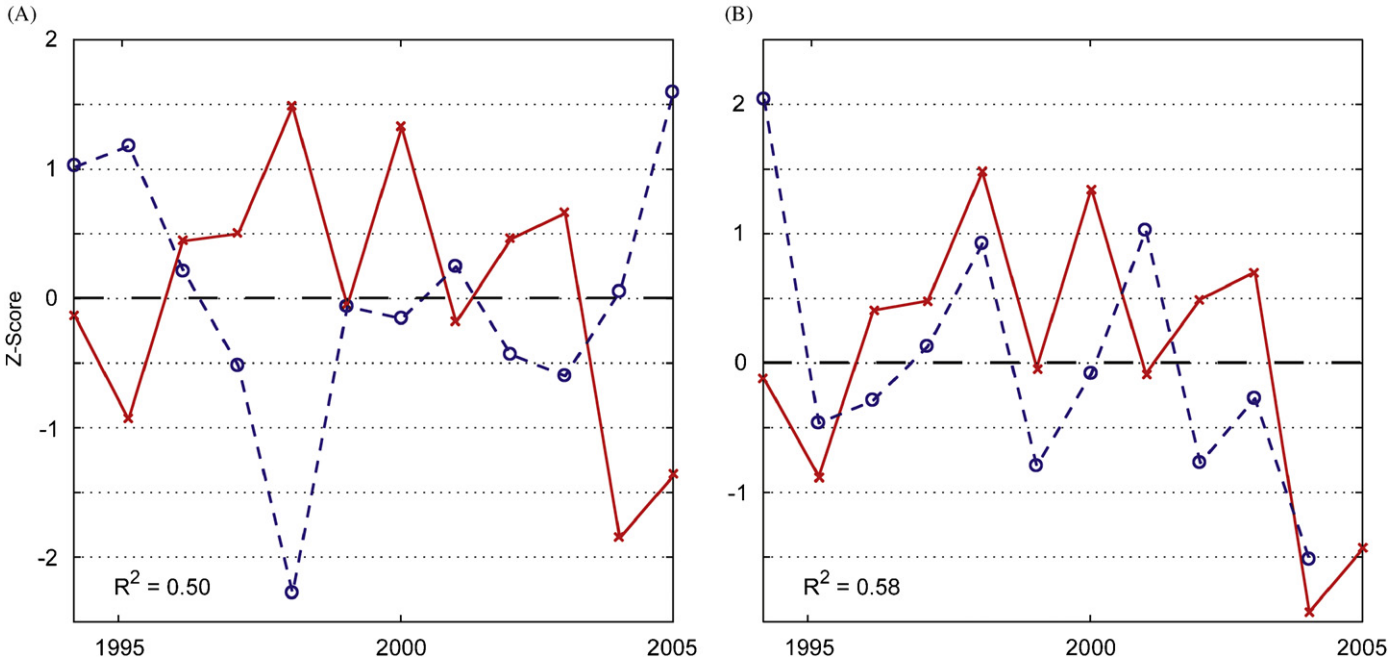

Fig. 10. Temporal correlations of first principal components of daily integrated primary production with ice and ocean ($r^2 \geqslant 0.5$). Due to the lag (see Methods section) the January 1996 cruise appears as 1995 in the *x*-axis, and so on. (A) Correlation between first principal component in primary production (blue) and first principal component in sea-ice retreat (red) with a combined variance of 50% explained, (B) temporal correlation of PC1 of sea-ice retreat (red) and SML (blue) with a combined variance of 58% explained. Correlation between first principal component in primary production and first principal component in summer mixed-layer depth not shown (combined variance of 14% explained). The *Z*-Score is the normalized value of the principal component eigenvalue, calculated for comparison purposes.

the mid-shelf, the inside of the 500 line, west of Renaud Island, and at mid-shelf and slope waters in the 300 line (areas shown blue in Fig. 11B). No or positive correlation was observed in other areas ($r = 0.2$–0.4).

3.3.3.2. Second mode of variability. The PCA can bring insight into the variability in primary production that correlated negatively with SML at mid-shelf. The second mode in primary production (explaining 11% of the total primary production variance) captured the response of phytoplankton in the outer shelf west of Adelaide Island (300 grid line) and at mid-shelf in the 500 line, where shallower mixed layers promoted higher primary production (and vice versa; Fig. 12B). Positive production mode (or enhanced production in the red and orange areas) was observed in 1997, 2000, 2005, and 2006 and negative mode in 1998, 2000, 2002, and 2003 (PC1; Fig. 12A). The spatial distribution of this second mode (i.e. EOF2) was seen also in the anomaly map for 2000 (Fig. 6). The temporal correlation of the second mode of primary production with the first mode of SML depth gives further evidence of the coupling between these two variables (Fig. 12C; $R^2 = 0.34$). The anomalies at the locations representative of the second mode (i.e. 200.130, 300.170, and 500.090 shown as red and yellow in Fig. 12B) showed that average-to-high primary production in 2000 and 2005 (Fig. 13A) was associated with negative (shallow) anomalies in SML (Fig. 13B) and high-to-neutral anomalies in the timing of sea-ice retreat (Fig. 13C).

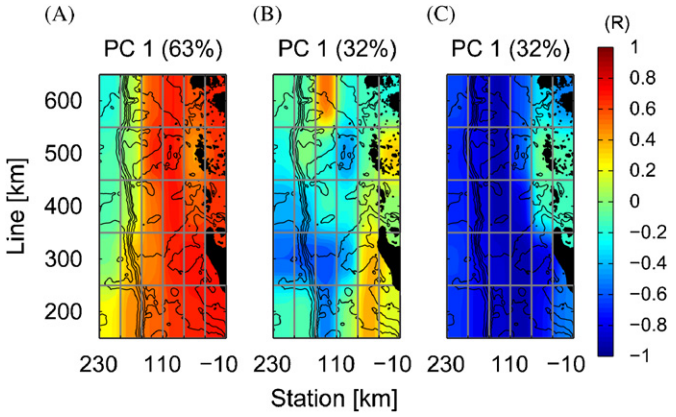

Fig. 11. Spatial correlation maps, where the time series of the first principal component of one variable is correlated with the time series of the anomalies of the second variable. Colors correspond to value of the correlation coefficient, with red indicating high positive correlation and blue, strong negative correlation. (A) Daily integrated primary production first principal component (explaining 63% of total variance) and anomalies of timing of sea-ice retreat; (B) summer mixed-layer depth first principal component (explaining 32% of SML variance) and anomalies of daily integrated primary production; and (C) summer mixed-layer depth first principal component (explaining 32% of SML variance) and anomalies of the timing of sea-ice retreat.

4. Discussion

The primary production in the wAP is related to sea-ice dynamics in several parameters of interest: intensity, location, and inter-annual variability. The area influenced by ice is responsible for the onshore–offshore gradient (Fig. 3A), and for the large inter-annual variability (factor of 7) in average production in summer (Fig. 3B). As rates were measured in January (no later than first week in February), the results in this study represent a snapshot of primary production at the height of the growth season (Arrigo et al., 1998). The importance of the study relies on its 12 consecutive years (1995–2006) in a $500 \times 200\,km^2$ grid area, with a resolution of ten to hundreds of km (i.e. mesoscale features). In particular, this study shows that to the first order, variability in production was largely explained by sea ice, particularly sea-ice retreat (Figs. 5A and 7A). The mechanism by which sea-ice retreat affects primary production, expected to be through the formation of a shallow mixed layer in surface waters as ice melts (Smith and Nelson, 1986), is more complex. The intensity of production was related to SML (Fig. 5B), while the variability around the mean at each location showed opposite dynamics in coastal and offshore waters (Fig. 7B). At these

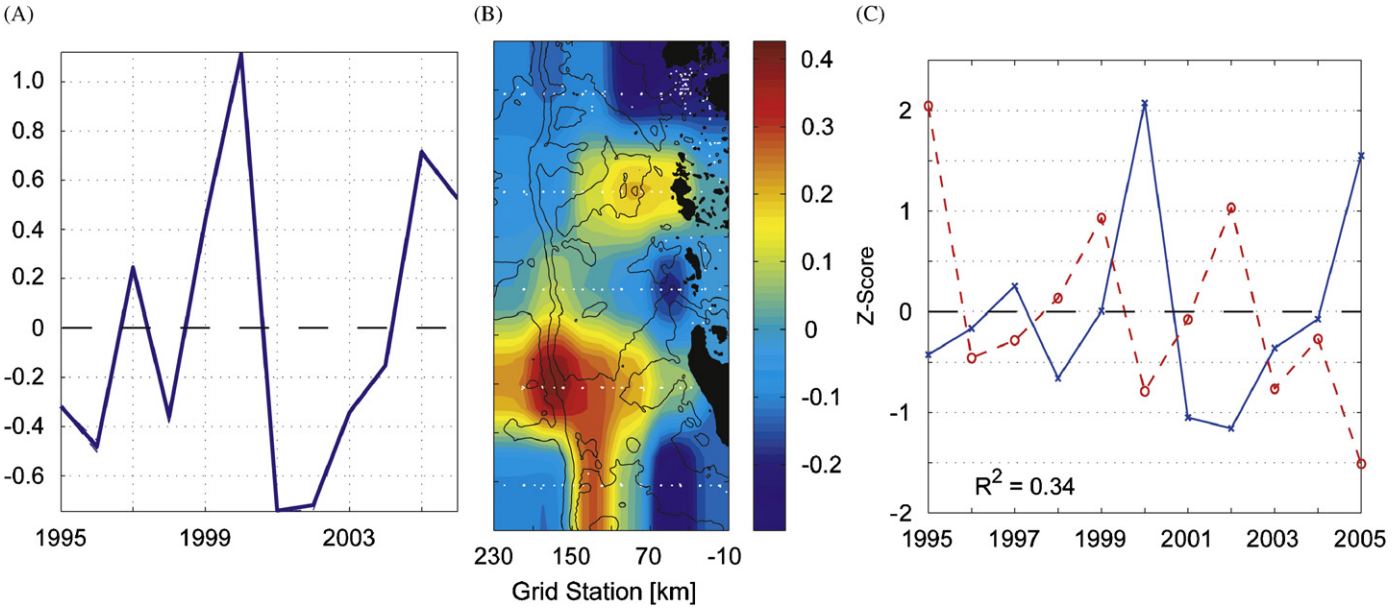

Fig. 12. Principal component analysis showing the second mode extracted in daily integrated primary production. (A) Time series of second principal component (PC2). (B) Second EOF (capturing 11% of variability in production) indicating the areas of variability in the years identified in PC2 (red areas show high production in 1997, 2000, 2005, and 2006 and low production in 1998, 2001, 2002, and 2003). The other areas (indicated in blue) present the opposite pattern; see year 2000 in Fig. 6 as an example. (C) Correlation between second principal component in primary production (red line) and first principal component in summer mixed-layer depth (blue line) with a combined variance of 34% explained of 34%. See the *Note* in Fig. 8.

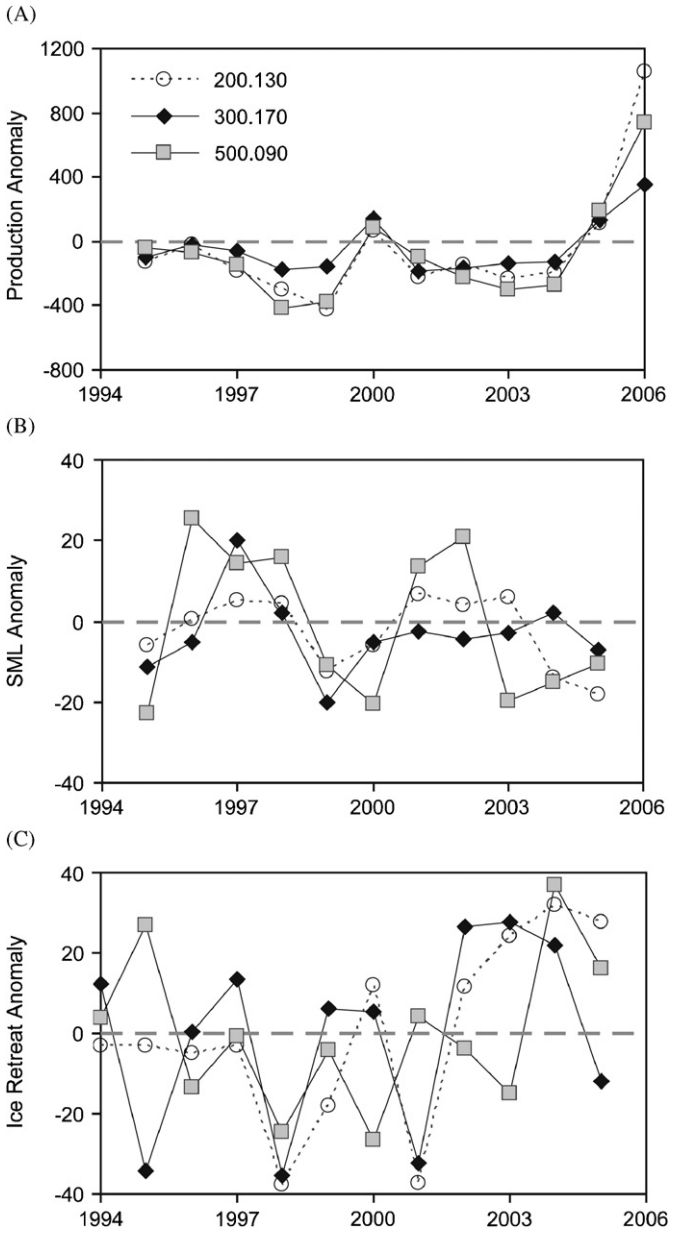

Fig. 13. Time series of the anomalies at three locations identified in mode 2 of the principal component analysis as explaining 11% of production variability in the region (see Fig. 12). (A) Daily integrated primary production; (B) summer mixed layer (SML); and (C) timing of sea-ice retreat. Positive anomalies in production in 2000, 2005, and 2006 (panel A) correlate with low (shallow) anomalies in mixed-layer depth (panel B) and late sea-ice retreat in 2005 and 2006 (panel C).

locations, the depth of the mixed layer seems to be defined by other factors then freshwater input from sea-ice retreat (Fig. 7C).

High biomass (i.e. chl *a*) accumulation in coastal waters in the wAP has been attributed to shallow mixed-layer depths (Mitchell and Holm-Hansen, 1991; Sakshaug et al., 1991; Schloss et al., 2002), usually o 25 m (Garibotti et al., 2005b). Experiments suggest that stratification in combination with seeding from sea-ice algae is needed for a sea-ice-edge bloom to develop (Giesenhagen et al., 1999). In this study we show that sea-ice melt during retreat is the mechanism that promotes high primary production, creating and maintaining shallow mixed layers in areas of high production. Although wind-driven water-column mixing processes can alter the response of phytoplankton to freshwater input and negate phytoplankton accumulation (Lancelot et al., 1991; Savidge et al., 1995), production at the sea-ice zones (SIZs), as described here, is responsible for ~22% of the primary production in the Southern Ocean (Arrigo et al., 1998). Similar high daily rates in primary production are found in other SIZ, the Weddell Sea–Scotia Sea (Smith and Nelson, 1990; Bracher et al., 1999), Ross Sea (Smith et al., 1996, 2000), as well as in the Arctic Seas (Engelsen et al., 2002; Hill and Cota, 2005).

4.1. Primary production and sea-ice dynamics

The retreat of sea ice on the western Antarctica Peninsula shelf, from early November to early February (Fig. 4B), is expected to be of importance to summer phytoplankton productivity, in the areas directly affected by the ice edge, the MIZ in January, or earlier in the season, the SIZ. The MIZ is described as an area of enhanced upper water-column stratification, which is conducive to phytoplankton accumulation (Smith and Nelson, 1985, 1986). In January, the presence of ice was constrained to coastal waters, east of Anvers and Renaud Island and to the southern half of Marguerite Bay. The rest of the study area can be better labeled as the SIZ (Tréguer and Jacques, 1992), where shallow SML have been modified by wave and wind action as well as solar heating since their formation.

The ice advances in fall or early winter (starting on average in late April in the most southern part of the grid) and advances northward over the next 5–6 months. Maximum ice, in terms of area covered (e.g., extent), occurs on average in August, and is then followed by a retreat over the next 5–6 months (Stammerjohn and Smith, 1996). The dynamics of sea-ice retreat on the wAP are complex in terms of timing as well as the amount of ice melted in any location. For example, ice thickness, influenced by wind (Stammerjohn et al., 2003), can actually increase during retreat due to mechanical processes, e.g., rafting and thickening. Spring of 2001 was anomalous in that showed an early retreat offshore was followed by a late retreat inshore (Massom et al., 2006). In addition, ice can retreat fast but late (2–3 months, i.e. year 1994), slow (6–7 months; year 2002), or a combination of fast and slow at different times of the retreat period. From hydrodynamic and dynamic forcing (variable wind events in direction and speed), we can expect a complex relationship between ice and phytoplankton distributions at the scales of analysis presented in this study (tens to hundreds of km).

4.1.1. Inter-annual variability

The time series in primary production defined a 5–6 year cycle with highs and lows varying by a factor of 7 (Fig. 3B). These rates are similar to those in the Ross Sea, where Smith et al. (2006) reported high inter-annual and spatial variability. In the 2001–2002 season the authors reported an average production of 0.70 g C m^{-2} d^{-1} (similar to the wAP average of 0.745 g C m^{-2} d^{-1}) and 1.82 g C m^{-2} d^{-1} for 2002–2003 (similar to 1.79 g C m^{-2} d^{-1} measured in January 2006).

A 5–6 year cycle in environmental forcing is the well-known El Niño/La Niña events in the equatorial Pacific. The effect of the 1997–1998 El Niño on worldwide primary production has been well documented (Behrenfeld et al., 2001). This event affected sea-ice dynamics (Stammerjohn et al., 2008), water masses (Meredith et al., 2004; Martinson et al., 2008), and chl *a* biomass in the eastern Belligshausen Sea (Smith et al., 2008). Three El Niño events occurred since 1995 (1994–1995, 1997–1998, and 2002–2003) and four La Niña events (1995–1996, 1998–1999, 1999–2000, and 2000–2001) using the NOAA Climate Prediction Center's definition. In general, high sea-level pressure (SLP) anomalies occur during El Niño, resulting in favorable ice conditions, e.g., late retreat, early advance, and vice versa for low SLP anomalies and La Niña (Martinson et al., 2008).

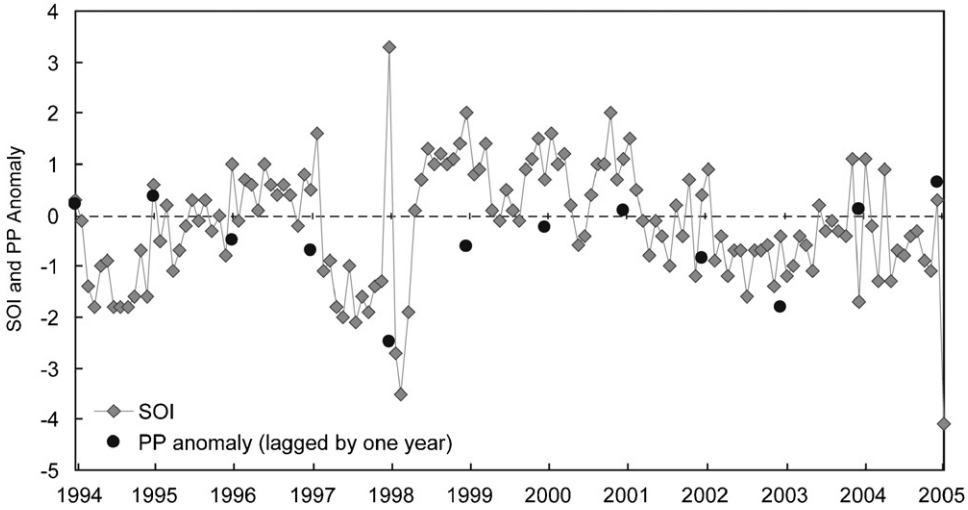

Fig. 14. Anomalies of average daily integrated primary production in the wAP in January ($n = 43$ stations, 1-year lag) compared with the time series of the time development of the Southern Oscillation Index, as monthly standard anomalies.

Furthermore, high-latitude response to La Niña brings persistent and/or stormy conditions, affecting the variability in sea-ice retreat (and advance; Stammerjohn et al., 2008). When northerly winds are persistent in November, the sea-ice retreat is anomalously early (e.g., 1991 and 2001) and when southerly winds dominate, the ice retreat is anomalously late (e.g., 2002; Stammerjohn et al., 2008).

The primary production in the wAP showed lower than average production in January of 1999 and 2004 (Fig. 14; note 1-year lag in primary production anomalies). During El Niño 1997–1998 event (negative SOI), there was early retreat along the coast (related to January primary production) and low primary production. This was also the case for El Niño 2002–2003, early retreat along the coast and low primary production in January 2003. For El Niño 1994–1995, the retreat was late everywhere, thus high January 1996 primary production. Other El Niño events do not show as clear pattern with production, which can be attributed to the complex mechanics of sea-ice retreat. For example, for January 1998, which showed low production, the spring 1997 retreat in the Palmer LTER area was late over the shelf but early along the coast. Spring 1997 had high-pressure atmospheric conditions and less storms, consistent with the high-latitude response to El Niño, so sea ice over the shelf slowly melted *in situ* (i.e. not being driven by wind toward the coast, where it would have mechanically thickened and taken longer to melt); instead once the sea ice melted over the shelf, it melted faster, i.e. earlier along the coast. Inconsistencies can be described also for La Niña events, where a late/early ice retreat offshore (eastern Bellinghausen Sea) is not related to the retreat along the coast. This is in contrast to the findings of Smith et al. (2008), where a more consistent relationship between phytoplankton biomass anomalies (as chl *a*) and ENSO was observed: early retreat during La Niña events coincided with lower than average chl *a* and vice versa for El Niño events. Several factors can explain the observed discrepancy. First, chl *a* anomalies strongly correlated with ENSO originate from offshore and shelf areas while the primary production anomalies are dominated by production in coastal waters. Second, and as pointed out by Smith and co-authors, inter-annual variability when sampling during a narrow window of time (e.g., month of January) can be amplified. Sampling in different years at fixed dates does not mean sampling at the same time of the seasonal cycle. By analyzing phytoplankton biomass during the growth season (October–March), it can be seen that the average "summer" production is highest during January, coincident with maximum solar irradiance, but maxima and minima on particular years can be observed early (i.e. December) or late (i.e. February). Finally, different responses to ENSO from chl *a* and primary production anomalies can be expected as different environmental drivers are known to affect biomass and production. While 68% of the production can be modeled from chl *a* biomass (Dierssen and Smith, 2000) another 32% of the primary production variance is not correlated with biomass and it is this component of the variance that can be independent from ENSO dynamics.

4.2. Primary production and summer mixed-layer depth

Freshwater input from melting sea ice is considered the major process in water-column stratification in the SIZ. Two factors are of importance: total amount of freshwater input to surface waters and the duration over which the input occurs, i.e. the time lapsed between ice melting and phytoplankton growth. In the wAP, the amount of freshwater in the (upper) SML is correlated to the length of the ice season (considered a proxy of ice volume; Stammerjohn et al., 2008). This correlation implies that the freshwater at any given location, and thus the degree of stratification, is a result of sea ice melting *in situ*. The exception is the inshore waters, where glaciers are considered an important source of freshwater input (Dierssen et al., 2002).

Although average productivity responds positively to average SML (Fig. 5B), the variability in primary production, in particular the very high production rates in coastal waters (positive anomalies) are related to deeper mixed layers (Fig. 7B). Only 11% of the variability in production, captured by the second mode in the PCA, is negatively related to mixed layers (Fig. 12). Later retreat in sea ice might be related to these shallower mixed layers at mid-shelf (Fig. 7C). The influence of large oceanographic features, such as the intrusion of the Upper Circumpolar Deep Water (UCDW) on to the shelf at the 300 grid line, can affect also the upper water-column stratification, as seen for 2002 (Martinson et al., 2008). Prézelin et al. (2000) suggested Eckman-driven upwelling in the inside of the 500 line, in the same location identified in the EOF2, a process that can affect SML depth. This feature was not observed in January 1994 (Prézelin et al., 2004). Our results suggest that a shallow SML at this location was seen only three times in the subsequent 12 years (St. 500.090 in Fig. 13).

4.2.1. Light adaptation in the summer mixed layer

As much as 63% of the variability in primary production (mode 1 in PCA), explaining inter-annual changes in regional production (Fig. 9), is related to deeper than average SMLs. A positive correlation between the anomalies of primary production and SML depth can be interpreted as a reversal of the effect of increased stratification in the spring, where a decrease in SML depth increases average irradiance. The establishment of a freshwater lens in surface waters is assumed to reduce light limitation originating from deep mixing, under conditions of low biomass (o 0.1 mg chl $a\,m^{-3}$ at the end of the winter).

After several months of growth and under conditions of low advection and/or grazing losses, phytoplankton abundance can become light limited due to self-shading. Representative examples of primary production positive anomalies correlating with SML are the inside stations of the 600 line (600.035) in 1996 and the inside of the 200 line (200.000) in 2002, which supported primary production in excess of 400 mg C $m^{-3}\,d^{-1}$ and 600 mg C $m^{-3}\,d^{-1}$, respectively (Fig. 15), with >20 mg chl $a\,m^{-3}$, a SML o 20 m, and an euphotic zone (Z_{eu}) of o 30 m (Fig. 16). In areas of high biomass accumulation, e.g., 30 mg m^{-3}, SML depth can vary by a factor of 4 (from 5 to 19 m) and Z_{eu} by a factor of ~2 (12–20 m). Further examination of the primary production at stations with high biomass shows a large variability in carbon uptake with depth, presumably due to different light environments. In 1996, a year of high coastal primary production, station 605.040 in the Anvers Island area (with 25 mg chl $a\,m^{-3}$, a SML of 19 m, Z_{eu} of 20.7 m, and excess macronutrients, 9.2 μM nitrate and 68.9 μM silicate) is contrasted with a station in Marguerite Bay (with 20 mg chl $a\,m^{-3}$, a SML 5 m, Z_{eu} of 12.5 m, 6.7 μM nitrate and 50.3 μM silicate). Non-limiting macronutrient concentration and assuming high micronutrients (Fe~7 nM in coastal waters of the wAP, Martin et al., 1990a, b) suggest irradiance as a limiting factor. Under conditions of phytoplankton being mixed down to the depth that can support effective photosynthesis, i.e. SML = Z_{eu}, production is maximum at the surface (>400 mg C $m^{-3}\,d^{-1}$) and phytoplankton can take advantage of high surface light (600.040 in Fig. 17). In contrast, when phytoplankton is constrained to

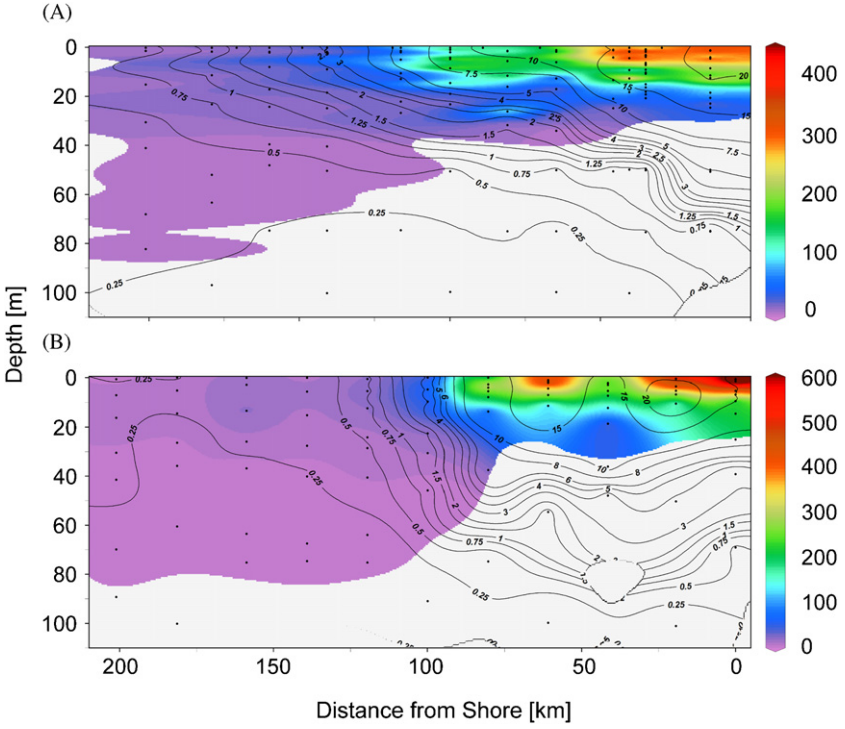

Fig. 15. Transect of primary production rates for (A) the 600 line in 1996 and (B) the 200 line in 2002. *X*-axis depicts distance from shore (km), *Y*-axis is depth (0–100 m), color shows rates of primary production in mg C $m^{-3}\,d^{-1}$ and contour lines describe the biomass in units of mg chl $a\,m^{-3}$. Primary production was determined to the depth of 1% surface PAR (euphotic zone).

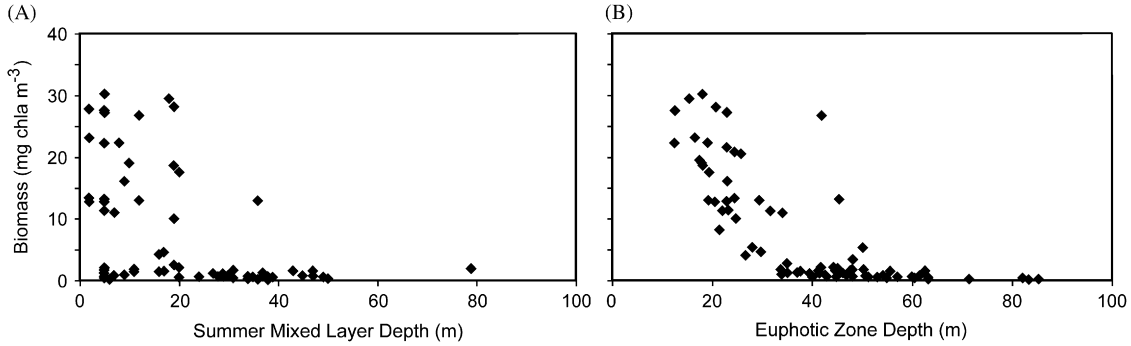

Fig. 16. Relationship between phytoplankton biomass (as concentration of chl *a* in mg m^{-3}) in 1996 and (A) SML (m) and (B) depth of euphotic zone (m), showing large accumulations (i.e. blooms) of >5 mg chl $a\,m^{-3}$ when SMLo 20 m.

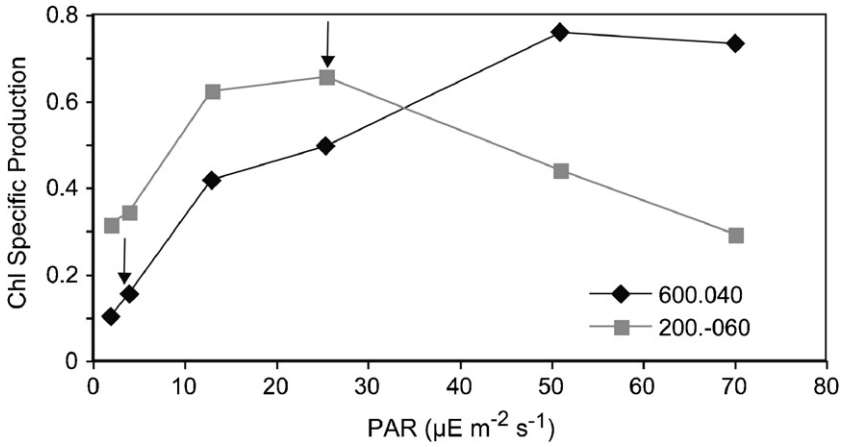

Fig. 17. Chlorophyll-specific primary production in coastal stations during January 1996, in mg C (mg chl *a*) h^{-1}, exposed to different light environments (different mixed layer and euphotic zone depths). Stations in the 600 line (station 600.040, black diamonds, located south of Anvers Island, Fig. 1) and in the 200 line (station 200.-060, gray squares, located in Marguerite Bay, Fig. 1). For the same irradiance in the water column (PAR or photosynthetically available radiation), 600.040 showed an integrated daily production of 4351 mg C m^{-2} d^{-1} and 200.-060 had 2354 mg C m^{-2} d^{-1}, and varying chl-specific production with depth, indicating adaptation to high- and low-light, respectively. Arrows indicate depth of summer mixed layer at each location.

a shallow 5-m SML it shows higher production at depth (PARo 20 μE m^{-2} s^{-1}) but lower primary production close to the surface (200.-060 in Fig. 17). Integrated production was 2.35 g C m^{-2} d^{-1} at 200.-060 and 4.31 g C m^{-2} d^{-1} at 600.040. In comparing photosynthetic efficiency, or production per unit chl *a* per hour, it can be seen that phytoplankton in Marguerite Bay found below the SML is more efficient than those at the same depth at 600.040, i.e. low-light adapted, but the surface phytoplankton within the SML, o 5 m, is less efficient, i.e. photo-inhibited. Deeper SML, closer to the Z_{eu}, allows for a more favorable overall light field at high chl *a* concentrations, supporting higher daily integrated primary production.

4.2.2. *Phytoplankton composition and variability in primary production*

Diatoms and cryptomonads are the dominant taxonomic groups in the wAP and responsible for most of the biomass present (Villafañe et al., 1993; Moline and Prezelin, 1996; Kang et al., 2001; Garibotti et al., 2003b), in particular large phytoplankton accumulations or blooms (Kozlowski, 2008). Production anomalies in these areas correlate positively with the dominance of diatoms ($r = 0.6$–0.8; Fig. 18). The opposite is true at mid-shelf, where the relative abundance of cryptomonads correlates with higher production anomalies ($r = -0.4$). A comparison with the correlation map of the primary production and SML anomalies (Fig. 7B) shows spatial similarity, i.e. diatom enrichment coincides with higher production and deeper SML and the dominance of cryptomonads coincides with higher production and shallower mixed layers at mid-shelf.

Comparison of our field data with cultures suggests that Antarctic diatoms will respond positively to an increase in irradiance within a deepening SML. Under conditions of abundant macro- and micronutrients, Antarctic diatoms exposed to a high irradiance of 90 μmol m^{-2} s^{-1} showed a chl-specific production of 1.66 mg C (mg chl *a*)$^{-1}$ h^{-1}, from a low of 0.59 mg C (mg chl *a*)$^{-1}$ h^{-1} at 20 μmol m^{-2} s^{-1} (van Oijen et al., 2004a, b). Similarly, the high-light-adapted phytoplankton from 600.040 had a surface chl-specific production of 0.74 mg C (mg chl *a*)$^{-1}$ h^{-1} at 70 μmol m^{-2} s^{-1} and ~0.45 mg C (mg chl *a*)$^{-1}$ h^{-1} at 20 μmol m^{-2} s^{-1} (Fig. 17). Somewhat lower estimates are expected in the field samples as these estimates are based on 24-h incubations and maximum production per chl *a* is considered to be

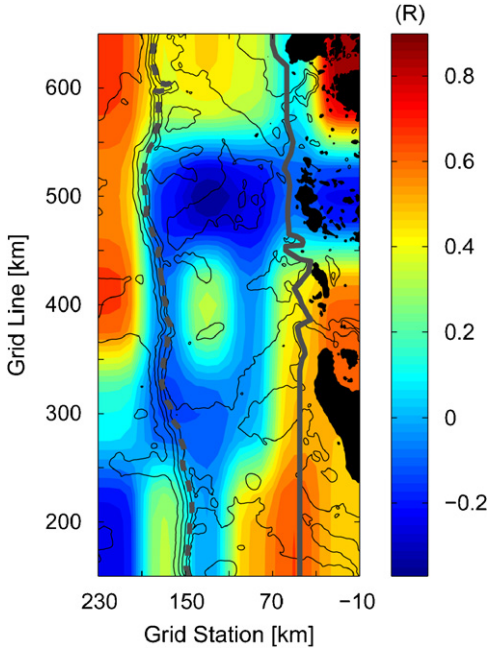

Fig. 18. Spatial correlation map: time series of anomalies of daily integrated primary production correlated with time series of anomalies of diatom:cryptomad ratio at each grid cell. Coastal and offshore areas show higher production with diatom dominance (red areas) while mid-shelf shows higher production with cryptomonad dominance (blue areas). Abundance of diatoms and cryptomonads was calculated based on photosynthetic pigments and the CHEMTAX method for chemotaxonomy (Kozlowski, 2008). Color bar shows the value of correlation coefficient (*R*).

1.1 mg C (mg chl *a*)$^{-1}$ h^{-1} (Holm-Hansen and Mitchell, 1991; Dierssen and Smith, 2000). The agreement between field and experimental data indicates that the diatoms will support higher daily water-column production under increased conditions of irradiance within the SML. Cell volume is another factor that could affect the degree of photo-adaptation in diatoms under conditions of high nutrients. For example, large diatoms, known to dominate in Marguerite Bay (Garibotti et al., 2003b), prefer low-light conditions (~20 μmol m^{-2} s^{-1}; Timmermans et al., 2001). Although not one single parameter in phytoplankton composition,

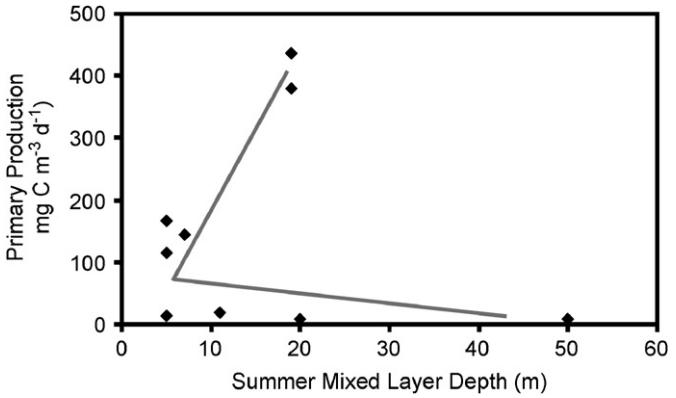

Fig. 19. Non-linear relationship between surface primary production and summer mixed-layer depth in the wAP. Example from line 600 during January 1996.

cell size, or photo-adaptation can explain the increased daily primary production under bloom conditions (chl $a > 20\,mg\,m^{-3}$) in the presence of deep SML, these results show a non-linear relationship between SML depth and primary production (i.e. Fig. 19), and extends our understanding of the environmental conditions that sustain high carbon uptake at the SIZ.

4.2.3. Micronutrients and mixed-layer depth

Other factors than sea ice are known to limit/enhance phytoplankton growth rate in Antarctic waters. In the open ocean, natural concentrations of Fe are considered limiting for most of the growth season. Under conditions of Fe addition, either in laboratory cultures or in the field, phytoplankton growth, in particular that of diatoms, is re-activated (Martin et al., 1990a; Boyd et al., 2000; Coale et al., 2004). Sometimes the response is modulated by light (Timmermans et al., 2001).

Seaward of the Antarctic Peninsula shelf, NW of Elephant Island, influx of nutrients from the permanent pycnocline into the overlying winter water is attributed to providing micronutrients to deep phytoplankton, where chl *a* maxima at 50–100 m have been shown to be photosynthetically active (Holm-Hansen and Hewes, 2004). Similarly, phytoplankton in slope waters of the wAP are thought to be enriched in diatoms under conditions of local upwelling, introducing micronutrients in the upper water column (Prézelin et al., 2000, 2004; Garibotti et al., 2003b). The presence of a chl *a* maximum in wAP slope waters suggests micronutrient limitation in upper waters during January (Garibotti et al., 2005b). In contrast, maximum chl *a* concentrations are found at/near the surface over the shelf and coastal waters.

Higher/lower production in slope waters when diatoms dominate/do not dominate (Figs. 7B and 18) can be attributed to entrainment of micronutrients to the upper water column by deepening of the SML. Similarly, upwelling bringing micronutrients to the inner shelf of the 500 line (500.090) in 2000 and 2005, as captured in the second mode of the PCA (Fig. 12), can explain higher production. Finally, the positive correlation between primary production and SML in coastal waters can be attributed to entrainment of micronutrients by deepening of the SML. The presence of diatoms, a decrease in light limitation, and higher production, as observed in the Palmer area in 1996 at St. 600.040 (Figs. 16 and 17), are all indicators of stress release, which can include micronutrients.

For Fe addition to enhance production as mixed layers deepen would require Fe limitation in surface waters. Martin et al. (1990a, b) measured 7 nM Fe in the Gerlache Strait (north of Anvers Island) and argued that it was more than enough to consume the 30 μM nitrate in the water column, at an uptake ratio of 5000:1 N:Fe. Fe limitation was found in open waters, with low Fe concentrations (~0.2 nM), 250 km away from the shelf break. In the wAP, any new input of Fe to the upper water column from depth brings macronutrients. Thus, only areas of low Fe concentration and high macronutrients are susceptible to Fe enrichment. Estimates of Fe concentration over the wAP shelf are needed to understand the possible mechanisms of production and diatom enhancement in the area. As a first approximation, Fe does not seem as limiting to regional average primary production in the wAP shelf as in the Ross Sea shelf (Sedwick et al., 2007).

4.3. Change of average primary production with time

Both the onshore–offshore gradient (average production) and the north–south gradient in variability in primary production observed in the wAP are correlated with sea-ice dynamics. The decrease in ice months in the area (Stammerjohn et al., 2008) is expected to affect coastal and shelf production during mid-summer. On the other hand, and as discussed previously, the dynamics of sea-ice retreat are complex and subject to great spatial and temporal variability in response to atmospheric conditions in the spring, making any prediction uncertain. Changes in sea-ice conditions could affect the average distribution of primary production in different ways. If sea-ice retreat occurs earlier or less freshwater melts in the area, the ecosystem could decrease the intensity of coastal production with a concomitant decrease in the gradient currently observed. Alternatively, the position of the gradient could move further inshore as the area of high production decreases in size. The overall result of any of these scenarios will be a decrease in primary production in the region at the height of the growth season, when higher potential production can be sustained by high solar irradiance and longer days.

Long-term changes in primary production can be measured by the slope of the time series of the anomalies (i.e. trend). The estimated long-term changes observed for the 12-year series are very low (Fig. 20), in the order of the estimated standard deviation values (Fig. 3A). A slight negative trend is observed in the Anvers Island area and a positive trend is seen toward the south, in coastal and shelf waters. Particular areas present increased primary production (see inserts) such as offshore in 500 and 300 grid lines and mid-shelf in the 200 grid line, but they are constrained to small-scale phenomena (40–80 km).

The lack of significant changes in primary production in the region (not statistically significant, $p > 0.05$) can be explained by a rapid adaptation of the system to new conditions. Although a decrease in summer sea ice might lead to a weakening of the SIZ in the wAP and a decrease in associated phytoplankton blooms, dominated by large, chain-forming diatoms such as those found in the MIZ in Marguerite Bay (Garibotti et al., 2005a), flagellate blooms (i.e. cryptomonad), such as the ones observed west of Anvers Island, can also maintain high rates of daily production (Fig. 3A). Thus, our present knowledge would support the hypothesis that further decreases in sea ice could affect the composition more than the total primary production in this area. Two factors support this conclusion. First, primary production in coastal waters of the Northern wAP (62–64°S) presents the onshore–offshore gradient (Smith et al., 1996) in spite of low number of days in winter sea ice, and thus low freshwater input (Stammerjohn et al., 2008). Second, high sea-ice persistence in Marguerite Bay is not correlated with summer production (Section 3.1), suggesting that the amount of freshwater input from sea ice does not correlate with local production. We further suggest that a linear change in primary production along

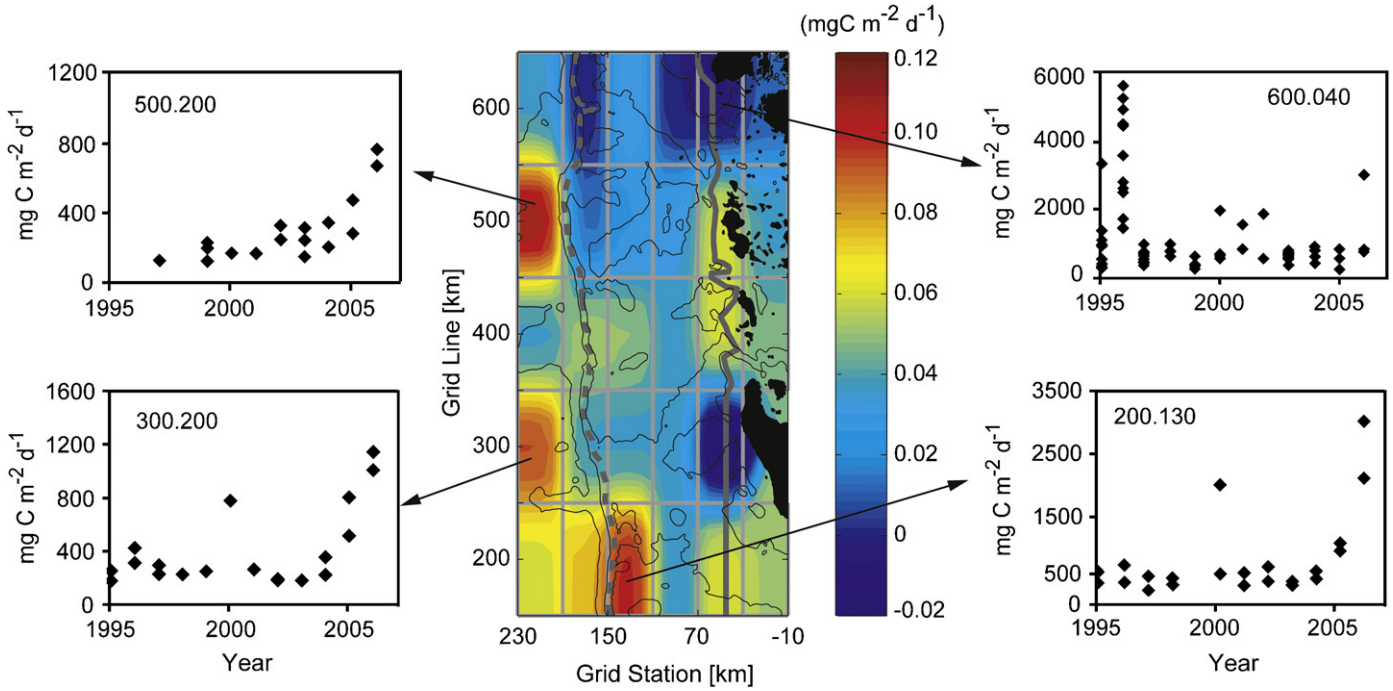

Fig. 20. Changes in mean primary production with time (trend) in the12-year series, calculated from the time series of anomalies at each location. Values in color bar are robust least squares linear regression coefficients. Insets depict time series of primary production rates at each of the locations in the grid that show positive or non-varying trend (in mg C m^{-2} d^{-1}). No cell showed significant trend, with significance estimated as slope/standard error of the fit >1.96.

a north–south gradient in the wAP is unlikely. Rather, as sea-ice melting in spring and summer moves south, we could expect maximum seasonal production to be maintained within an optimum location, with lower production north due to decreased sea-ice presence and lower toward the south due to decreased solar input (lower sun angles).

The impact that a change in phytoplankton composition in coastal waters might have on the classic Antarctic diatom-krill-whale food chain is yet unclear (Quetin et al., 2007). Diatom-rich waters also can be found associated with fronts, e.g., in wAP slope waters (Prézelin et al., 2000; Varela et al., 2002; Garibotti et al., 2003a) and this feature could become more important with time. However, transition from diatoms to flagellates could affect the spatial distribution of krill in nearshore waters (Walsh et al., 2001). Any change in phytoplankton composition affects not only adult krill but also young 1-year krill, found in late spring (October and November), which are known to prefer diatoms (Ross et al., 2000).

4.4. Relationship with the eastern Bellingshausen Sea

Pigment biomass (as chl *a*) over the greater wAP region, and including the eastern Bellingshausen Sea, showed spatial and temporal variability in response to sea ice and wind forcing (Smith et al., 2008). The spring bloom in the region starts offshore of slope waters in early spring, ~300 km offshore. The timing of the spring sea-ice retreat has some associations with when and where the phytoplankton blooms occur (as seen for the shelf), but these associations are not always consistent across the wAP region, particularly off-to-onshore, and over spring–summer. For example, the sea-ice retreat was late during October–November in 1997 and 2002 (i.e. was still over the SACCF region in November), and consequently the offshore spring bloom did not occur. Subsequent to the late retreat offshore, the retreat over the inshore shelf area was early (relative to the mean retreat time in this location), and chl *a* biomass concentrations over the shelf were low in January–February of 1998 and 2003, presumably due to a lack of a well-developed ice-edge bloom at the height of the growth season. Therefore, a late sea-ice retreat offshore of the shelf break region and an early retreat over the inshore shelf region were both associated with low pigment biomass in both of these locations.

In contrast, the retreat in 1995 and 2001 was early offshore and late inshore, and subsequently the chl *a* concentrations (and primary production) in January 1996 and 2002 were two of the highest summer averages measured within the wAP (Fig. 3B). The pigment biomass concentrations also were high offshore of the shelf break in 2001. In further contrast, the lowest chl *a* concentrations detected within the Palmer LTER area were in January 1999 and prior to that the spring retreat were early across the entire wAP region. Despite the low concentrations detected over the shelf in January 1999, a well-developed offshore bloom started as early as October (in fact the only October in the 1997–2003 time period to show a bloom), presumably in response to the anomalously earlier sea-ice retreat for this location. Therefore, the associations between anomalies in the timing of the spring sea-ice retreat and phytoplankton biomass concentration are spatially and seasonally different between shelf and offshore regions. In general, an early sea-ice retreat over the region offshore of the shelf break favors a spring bloom in this location (e.g., a strong SACCF influence promotes phytoplankton growth), whereas a later sea-ice retreat over the shelf and along the coast favors a summer bloom closer inshore.

5. Summary and conclusions

Average primary production rates in the wAP can vary by an order of magnitude, from ~250 to ~1100 mg C m^{-2} d^{-1}. A strong onshore–offshore gradient is evident along the peninsula with higher production inshore. Shelf production presents intermediate values of ~500 to 750 mg C m^{-2} d^{-1}. Over the

continental slope, daily integrated production rates are between 250 and 400 mg C m^{-2} d^{-1}. Summer primary production in space and time is associated with the timing of sea-ice retreat over the inner shelf. In contrast, production in slope waters is not related to sea-ice retreat (see also Smith et al., 2006). Sea-ice melting delivers freshwater onto surface waters, strengthening stratification and decreasing the depth of the SML. Average production is higher in coastal and inner shelf areas, where the mixed layer is shallow (5–25 m). The deepening of the average mixed layer toward the slope establishes the onshore–offshore gradient in average production.

The first two modes determined by principal component analysis (PCA) explain approximately 72% of the variability in primary production. The first mode (62% of the variance) captures the inter-annual variability in production and it is loosely correlated with ENSO dynamics (i.e. SOI), presumably due to the complexity of the timing of sea-ice retreat over the shelf. The variability in production in this mode is correlated with a deepening of the SMLs in coastal and slope waters, in contrast to the relationship measured for average rates. A deepening of SMLs in coastal waters can provide enhanced light field to large phytoplankton accumulations that become self-shading. The second mode (11% of the variance) captures variability in production associated at mid-shelf and, similar to the average primary production, it is associated negatively with shallow mixed layers.

No significant trend in primary production anomalies was observed in the 12 years of study. The high inter-annual variability (factor of 7) shown in this study suggests that any trends in regional primary production might be difficult to determine in this area and will necessitate a longer time series.

Acknowledgments

The authors thank the many collaborators, technicians, and volunteers to the Palmer LTER program for data collection and analysis (1994–2007); L. Yarmey and K. Pistone for technical help in manuscript preparation. The authors gratefully acknowledge the support of Antarctic Support Associates (1994–1999) and Raytheon Polar Services (2000–2007) for logistical support in the field and to the captains and crew of the R.V. *Polar Duke* (1995–1997) and ARSV *Laurence M. Gould* (1998–2006). NCEP/NCAR re-analysis data were acquired from NOAA via http://www.cdc.noaa.gov/cdc/reanalysis/reanalysIslandshtml. SSM/I data were obtained from the NASA Earth Observing System Distributed Active Archive Center (DAAC) at the US National Snow and Ice Data Center, University of Colorado, Boulder. Fig. 15 was generated using Ocean Data View, Schlitzer, R., http://www.awi-bremerhaven.de/GEO/ODV, 2005. This project was funded by NSF Awards OPP90-11927, OPP96-32763, OPP-0217282 and the NSF support is gratefully acknowledged. This paper is Palmer LTER Contribution no. 0305.

References

Ackley, S.F., Sullivan, C.W., 1994. Physical controls on the development and characteristics of Antarctic sea-ice biological communities—a review and synthesis. Deep-Sea Research I 41, 1583–1604.

Aitchison, J., 1955. On the distribution of a positive random variable having a discrete probability mass at the origin. Journal of the American Statistical Association 50, 901–908.

Aitchison, J., Brown, J.A.C., 1957. The Lognormal Distribution. Cambridge University Press, Cambridge.

Arrigo, K.R., Worthen, D., Schnell, A., Lizotte, M.P., 1998. Primary production in Southern Ocean waters. Journal of Geophysical Research—Oceans 103, 15587–15600.

Behrenfeld, M.J., Randerson, J.T., McClain, C.R., Feldman, G.C., Los, S.O., Tucker, C.J., Falkowski, P.G., Field, C.B., Frouin, R., Esaias, W.E., Kolber, D.D., Pollack, N.H., 2001. Biospheric primary production during an ENSO transition. Science 291, 2594–2597.

Boyd, P.W., Robinson, C., Savidge, G., Williams, P.J., 1995. Water column and sea-ice primary production during Austral spring in the Bellingshausen Sea. Deep-Sea Research II 42, 1177–1200.

Boyd, P.W., Watson, A.J., Law, C.S., Abraham, E.R., Trull, T., Murdoch, R., Bakker, D.C.E., Bowie, A.R., Buesseler, K.O., Chang, H., Charette, M., Croot, P., Downing, K., Frew, R., Gall, M., Hadfield, M., Hall, J., Harvey, M., Jameson, G., LaRoche, J., Liddicoat, M., Ling, R., Maldonado, M.T., McKay, R.M., Nodder, S., Pickmere, S., Pridmore, R., Rintoul, S., Safi, K., Sutton, P., Strzepek, R., Tanneberger, K., Turner, S., Waite, A., Zeldis, J., 2000. A mesoscale phytoplankton bloom in the polar Southern Ocean stimulated by iron fertilization. Nature 407, 695–702.

Bracher, A.U., Kroon, B.M.A., Lucas, M.I., 1999. Primary production, physiological state and composition of phytoplankton in the Atlantic sector of the Southern Ocean. Marine Ecology Progress Series 190, 1–16.

Burkill, P.H., Edwards, E.S., Sleigh, M.A., 1995. Microzooplankton and their role in controlling phytoplankton growth in the marginal ice zone of the Bellingshausen sea. Deep-Sea Research Part II 42 (4-5), 1277–1290.

Carrillo, C.J., Karl, D.M., 1999. Dissolved inorganic carbon pool dynamics in northern Gerlache Strait, Antarctica. Journal of Geophysical Research—Oceans 104, 15873–15884.

Coale, K.H., Johnson, K.S., Chavez, F.P., Buesseler, K.O., Barber, R.T., Brzezinski, M.A., Cochlan, W.P., Millero, F.J., Falkowski, P.G., Bauer, J.E., Wanninkhof, R.H., Kudela, R.M., Altabet, M.A., Hales, B.E., Takahashi, T., Landry, M.R., Bidigare, R.R., Wang, X.J., Chase, Z., Strutton, P.G., Friederich, G.E., Gorbunov, M.Y., Lance, V.P., Hilting, A.K., Hiscock, M.R., Demarest, M., Hiscock, W.T., Sullivan, K.F., Tanner, S.J., Gordon, R.M., Hunter, C.N., Elrod, V.A., Fitzwater, S.E., Jones, J.L., Tozzi, S., Koblizek, M., Roberts, A.E., Herndon, J., Brewster, J., Ladizinsky, N., Smith, G., Cooper, D., Timothy, D., Brown, S.L., Selph, K.E., Sheridan, C.C., Twining, B.S., Johnson, Z.I., 2004. Southern ocean iron enrichment experiment: carbon cycling in high- and low-Si waters. Science 304, 408–414.

Comiso, J.C., 1995. Sea-ice geophysical parameters from SMMR and SSM/I data. In: Ikeda, M., Dobson, F.W. (Eds.), Oceanographic Applications of Remote Sensing. CRC Press, Boca Raton, FL, pp. 321–338.

Comiso, J.C., Cavalieri, D.J., Parkinson, C.L., Gloersen, P., 1997. Passive microwave algorithms for sea ice concentration: a comparison of two techniques. Remote Sensing of Environment 60, 357–384.

Dierssen, H.M., Smith, R.C., 2000. Bio-optical properties and remote sensing ocean color algorithms for Antarctic Peninsula waters. Journal of Geophysical Research 105, 26301–26312.

Dierssen, H.M., Smith, R.C., Vernet, M., 2001. Long term observations of meltwater and biomass in Antarctic coastal waters. American society of limnology and oceanography, aquatic sciences 2001. EOS, transactions, American geophysical union, Albuquerque, NM.

Dierssen, H.M., Smith, R.C., Vernet, M., 2002. Glacial meltwater dynamics in coastal waters West of the Antarctic Peninsula. Proceedings of the National Academy of Sciences 99, 1790–1795.

Engelsen, O., Hegseth, E.N., Hop, H., Hansen, E., Falk-Petersen, S., 2002. Spatial variability of chlorophyll-a in the marginal ice zone of the Barents Sea, with relations to sea ice and oceanographic conditions. Journal of Marine Systems 35, 79–97.

Fritsen, C.H., Ackley, S.F., Kremer, J.N., Sullivan, C.W., 1998. Flood–freeze cycles and microalgal dynamics in Antarctic pack ice. In: Lizotte, M., Arrigo, K. (Eds.), Antarctic Sea Ice: Biological Processes, Interactions and Variability. American Geophysical Union, Washington, DC.

Garibotti, I.A., Vernet, M., Ferrario, M.E., Smith, R.C., Ross, R.M., Quetin, L.B., 2003a. Phytoplankton spatial distribution in the western Antarctic Peninsula (Southern Ocean). Marine Ecology Progress Series 261, 21–39.

Garibotti, I.A., Vernet, M., Kozlowski, W.A., Ferrario, M.E., 2003b. Composition and biomass of phytoplankton assemblages in coastal Antarctic waters: a comparison of chemotaxonomic and microscopic analyses. Marine Ecology Progress Series 247, 27–42.

Garibotti, I.A., Vernet, M., Ferrario, M.E., 2005a. Annually recurrent phytoplanktonic assemblages during summer in the seasonal ice zone west of the Antarctic Peninsula (Southern Ocean). Deep-Sea Research I 52, 1823–1841.

Garibotti, I.A., Vernet, M., Smith, R.C., Ferrario, M.E., 2005b. Interannual variability in the distribution of the phytoplankton standing stock across the seasonal sea-ice zone west of the Antarctic Peninsula. Journal of Plankton Research 27, 825–843.

Garrison, D.L., Ackley, S.F., Buck, K.R., 1983. A physical-mechanism for establishing algal populations in Frazil ice. Nature 306, 363–365.

Giesenhagen, H.C., Detmer, A.E., de Wall, J., Weber, A., Gradinger, R.R., Jochem, F.J., 1999. How are Antarctic planktonic microbial food webs and algal blooms affected by melting of sea ice? Microcosm simulations. Aquatic Microbial Ecology 20, 183–201.

Gilbert, R.O., 1987. Characterizing lognormal populations. In: Statistical Methods for Environmental Pollution Monitoring. Van Nostrand Reinhold, New York (Chapter 13).

Hill, V., Cota, G., 2005. Spatial patterns of primary production on the shelf, slope and basin of the Western Arctic in 2002. Deep-Sea Research II 52, 3344–3354.

Holm-Hansen, O., Hewes, C.D., 2004. Deep chlorophyll-a maxima (DCMs) in Antarctic waters-I. Relationships between DCMs and the physical, chemical, and optical conditions in the upper water column. Polar Biology 27 (11), 699–710.

Holm-Hansen, O., Mitchell, B.G., 1991. Spatial and temporal distribution of phytoplankton and primary production in the western Bransfield Strait region. Deep-Sea Research 38, 961–980.
Kang, S.H., Kang, J.S., Lee, S., Chung, K.H., Kim, D., Park, M.G., 2001. Antarctic phytoplankton assemblages in the marginal ice zone of the northwestern Weddell Sea. Journal of Plankton Research 23 (4), 333–352.
Kaplan, A., Kushnir, Y., Cane, M.A., Blumenthal, M.B., 1997. Reduced space optimal analysis for historical data sets: 136 years of Atlantic sea surface temperatures. Journal of Geophysical Research—Oceans 102, 27835–27860.
Klinck, J.M., 1998. Heat and salt changes on the continental shelf west of the Antarctic Peninsula between January 1993 and January 1994. Journal of Geophysical Research 103, 7617–7636.
Kozlowski, W.A., 2008. Pigment derived phytoplankton composition along the Western Antarctic Peninsula. Thesis, Master of Science, San Diego State University.
Lancelot, C., Billen, G., Veth, C., Becquevort, S., Mathot, S., 1991. Modeling carbon cycling through phytoplankton and microbes in the Scotia–Weddell Sea area during sea ice retreat. Marine Chemistry 35, 305–324.
Lancelot, C., Mathot, S., Veth, C., Debaar, H., 1993. Factors controlling phytoplankton ice-edge blooms in the marginal ice-zone of the Northwestern Weddell sea during sea-ice retreat 1988 — field observations and mathematical-modeling. Polar Biology 13 (6), 377–387.
Martin, J.H., Fitzwater, S.E., Gordon, R.M., 1990a. Iron deficiency limits phytoplankton growth in Antarctic waters. Global Biogeochemical Cycles 4, 5–12.
Martin, J.H., Gordon, R.M., Fitzwater, S.E., 1990b. Iron in Antarctic waters. Nature 345, 156–158.
Martinson, D.G., Stammerjohn, S., Iannuzzi, R.A., Smith, R.C., Vernet, M., 2008. Palmer, Antarctica, long term ecological research program first twelve years: physical oceanography, spatio-temporal variability. Deep-Sea Research II, this issue [doi:10.1016/j.dsr2.2008.04.038].
Massom, R., Stammerjohn, S., Smith, R.C., Pook, Iannuzzi, R., Adams, Martinson, D., Vernet, M., Fraser, W., Quetin, L., Ross, R., Massom, Y., Krouse, 2006. Extreme anomalous atmospheric circulation in the West Antarctic Peninsula region in Austral spring and summer 2001/2, and its profound impact on sea ice and biota. Journal Climate Research 19, 3544–3571.
Meredith, M.P., Renfrew, I.A., Clarke, A., King, J.C., Brandon, M.A., 2004. Impact of the 1997/98 ENSO on upper-ocean characteristics in Marguerite Bay, western Antarctic Peninsula. Journal Geophysical Research—Oceans 109, L21305.
Mitchell, B.G., Holm-Hansen, O., 1991. Observations and modeling of the Antarctic phytoplankton crop in relation to mixing depth. Deep-Sea Research 38, 981–1007.
Moline, M.A., Prezelin, B.B., 1996. Palmer LTER 1991–1994: long-term monitoring and analyses of physical factors regulating variability in coastal Antarctic phytoplankton biomass, in situ productivity and taxonomic composition over subseasonal, seasonal and interannual time scales phytoplankton dynamics. Marine Ecology Progress Series 145 (1–3), 143–160.
Moore, J.K., Abbott, M.R., 2000. Phytoplankton chlorophyll distributions and primary production in the Southern Ocean. Journal of Geophysical Research-Oceans—Oceans 105, 28709–28722.
Pennington, M., 1983. Efficient estimators of abundance, for fish and plankton surveys. Biometrics 39, 281–286.
Prézelin, B.B., Hofmann, E.E., Mengelt, C., Klinck, J.M., 2000. The linkage between upper circumpolar deep water (UCDW) and phytoplankton assemblages on the west Antarctic Peninsula continental shelf. Journal of Marine Research 58, 165–202.
Prézelin, B.B., Hofmann, E.E., Moline, M., Klinck, J.M., 2004. Physical forcing of phytoplankton community structure and primary production in continental shelf waters of the Western Antarctic Peninsula. Journal of Marine Research 62, 419–460.
Quetin, L.B., Ross, R.M., Fritsen, C.H., Vernet, M., 2007. Ecological responses of Antarctic krill to environmental variability: can we predict the future? Antarctic Science 19 (2), 253–266.
Ross, R.M., Quetin, L.B., Baker, K.S., Vernet, M., Smith, R.C., 2000. Growth limitation in young Euphausia superba under field conditions. Limnology and Oceanography 45, 31–43.
Sakshaug, E., Slagstad, D., Holm-Hansen, O., 1991. Factors controlling the development of phytoplankton blooms in the Antarctic Ocean—a mathematical model. Marine Chemistry 35, 259–271.
Savidge, G., Harbour, D.S., Gilpin, L.C., Boyd, P.W., 1995. Phytoplankton distributions and production in the Bellingshausen Sea, Austral spring 1992. Deep-Sea Research II 42, 1201–1224.
Schloss, I.R., Ferreyra, G.A., Ruiz-Pino, D., 2002. Phytoplankton biomass in Antarctic shelf zones: a conceptual model based on Potter Cove, King George Island. Journal of Marine Systems 36, 129–143.
Sedwick, P.N., Garcia, N.S., Riseman, S.F., Marsay, C.M., DiTullio, G.R., 2007. Evidence for high iron requirements of colonial *Phaeocystis antarctica* at low irradiance. Biogeochemistry 83 (1–3), 83–97.
Smith, R.C., Dierssen, H.M., Vernet, M., 1996. Phytoplankton biomass and productivity in the western Antarctic Peninsula region. In: Ross, R.M., Hofmann, E.E., Quetin, L.B. (Eds.), Foundations for Ecological Research West of the Antarctic Peninsula. American Geophysical Union, Washington, DC.
Smith, R.C., Baker, K.S., Byers, M.L., Stammerjohn, S.E., 1998a. Primary productivity of the Palmer Long Term Ecological Research Area and the Southern Ocean. Journal of Marine Systems 17, 245–259.
Smith, R.C., Baker, K.S., Vernet, M., 1998b. Seasonal and interannual variability of phytoplankton biomass west of the Antarctic Peninsula. Journal of Marine Systems 17, 229–243.
Smith, R.C., Baker, K.S., Dierssen, H.M., Stammerjohn, S.E., Vernet, M., 2001. Variability of primary production in an Antarctic marine ecosystem as estimated using a multi-scale sampling strategy. American Zoologist 41, 40–56.
Smith, R.C., Fraser, W.R., Stammerjohn, S.E., Vernet, M., 2003. Palmer Long-Term Ecological Research on the Antarctic Marine Ecosystem. In: Domack, E., Leventer, A., Burnett, A., Bindschadler, R., Convey, P., Kirby, M. (Eds.), Antarctic Peninsula Climate Variability: Historical and Paleoenvironmental Perspective. American Geophysical Union, Washington, DC, pp. 131–144.
Smith, R.C., Martinson, D.G., Stammerjohn, S.E., Iannuzzi, R.A., Ireson, K., 2008. Bellingshausen and Western Antarctic Peninsula region: pigment biomass and sea ice spatial/temporal distributions and interannual variability. Deep Sea Research II, this issue [doi:10.1016/j.dsr2.2008.04.027].
Smith, W.O., Nelson, D.M., 1985. Phytoplankton bloom produced by receding ice edge in the Ross Sea: spatial coherence with the density field. Science 227, 163–165.
Smith, W.O., Nelson, D.M., 1986. Importance of ice edge phytoplankton production in the Southern-Ocean. Bioscience 36, 251–257.
Smith, W.O., Nelson, D.M., 1990. Phytoplankton growth and new production in the Weddell Sea marginal ice-zone in the Austral Spring and Autumn. Limnology and Oceanography 35 (4), 809–821.
Smith, W.O., Baumann, M.E.M., Wilson, D.L., Aletsee, L., 1987. Phytoplankton biomass and productivity in the marginal ice-zone of the Fram Strait during summer 1984. Journal of Geophysical Research—Oceans 92, 6777–6786.
Smith, W.O., Marra, J., Hiscock, M.R., Barber, R.T., 2000. The seasonal cycle of phytoplankton biomass and primary productivity in the Ross Sea, Antarctica. Deep-Sea Research II 47, 3119–3140.
Smith, W.O., Shields, A.R., Peloquin, J.A., Catalano, G., Tozzi, S., Dinniman, M.S., Asper, V.A., 2006. Interannual variations in nutrients, net community production, and biogeochemical cycles in the Ross Sea. Deep-Sea Research II 53, 815–833.
Stammerjohn, S.E., Smith, R.C., 1996. Spatial and temporal variability of western Antarctic Peninsula sea ice coverage. In: Ross, R.M., Hofmann, E.E., Quetin, L.B. (Eds.), Foundations for Ecological Research West of the Antarctic Peninsula. American Geophysical Union, Washington, DC, pp. 81–104.
Stammerjohn, S.E., Drinkwater, M.R., Smith, R.C., Liu, X., 2003. Ice–atmosphere interactions during sea-ice advance and retreat in the western Antarctic Peninsula region. Journal of Geophysical Research 108, 3329–3344.
Stammerjohn, S.E., Martinson, D.G., Smith, R.C., Iannuzzi, R.A., 2008. Sea ice in the Western Antarctic Peninsula region: spatio-temporal variability from ecological and climate change perspectives. Deep Sea Research II, this issue [doi:10.1016/j.dsr2.2008.04.026].
Timmermans, K.R., Davey, M.S., van der Wagt, B., Snoek, J., Geider, R.J., Veldhuis, M.J.W., Gerringa, L.J.A., de Baar, H.J.W., 2001. Co-limitation by iron and light of *Chaetoceros brevis*, C-dichaeta and C-calcitrans (Bacillariophyceae). Marine Ecology Progress Series 217, 287–297.
Tréguer, P., Jacques, G., 1992. Dynamics of nutrients and phytoplankton, and fluxes of carbon, nitrogen, and silicon in the Antarctic Ocean. Polar Biology 12, 149–162.
van Oijen, T., van Leeuwe, M.A., Gieskes, W.W.C., De Baar, H.J.W., 2004a. Effects of iron limitation on photosynthesis and carbohydrate metabolism in the Antarctic diatom Chaetoceros brevis (Bacillariophyceae). European Journal of Phycology 39 (2), 161–171.
van Oijen, T., van Leeuwe, M.A., Granum, E., Weissing, F.J., Bellerby, R.G.J., Gieskes, W.W.C., de Baar, H.J.W., 2004b. Light rather than iron controls photosynthate production and allocation in Southern Ocean phytoplankton populations during austral autumn. Journal of Plankton Research 26 (8), 885–900.
Varela, M., Fernandez, E., Serret, P., 2002. Size-fractionated phytoplankton biomass and primary production in the Gerlache and south Bransfield Straits (Antarctic Peninsula) in Austral summer 1995–1996. Deep-Sea Research II 49, 749–768.
Vernet, M., Smith, R.C., 2006. Measuring and modelling primary production in marine pelagic ecosystems. In: Fahey, J., Knapp, A. (Eds.), LTER Net Primary Production Methods. Oxford University Press, Oxford.
Villafañe, V., Helbling, E.W., Holm-Hansen, O., 1993. Phytoplankton around Elephant Island, Antarctica. Polar Biology 13 (3), 183–191.
Walsh, J.J., Dieterle, D.A., Lenes, J., 2001. A numerical analysis of carbon dynamics of the Southern Ocean phytoplankton community: the roles of light and grazing in effecting both sequestration of atmospheric CO_2 and food availability to larval krill. Deep-Sea Research I 48, 1–48.
Waters, K.J., Smith, R.C., 1992. Palmer LTER: a sampling grid for the Palmer LTER program. Antarctic Journal of the United States 27, 236–239.